

Physiologically based pharmacokinetic (PBPK) modeling of the role of CYP2D6 polymorphism for metabolic phenotyping with dextromethorphan

Jan Grzegorzewski^{1*}, Janosch Brandhorst¹ and Matthias König¹

¹ Institute for Theoretical Biology, Institute of Biology, Humboldt University, Berlin, Germany

Correspondence*:

Jan Grzegorzewski
grzegorj@hu-berlin.de

2 ABSTRACT

The cytochrome P450 2D6 (CYP2D6) is a key xenobiotic-metabolizing enzyme involved in the clearance of many drugs. Genetic polymorphisms in CYP2D6 contribute to the large inter-individual variability in drug metabolism and could affect metabolic phenotyping of CYP2D6 probe substances such as dextromethorphan (DXM). To study this question, we (i) established an extensive pharmacokinetics dataset for DXM; and (ii) developed and validated a physiologically based pharmacokinetic (PBPK) model of dextromethorphan (DXM) and its metabolites dextrorphan (DXO) and dextrorphan O-glucuronide (DXO-Glu) based on the data. Drug-gene interactions (DGI) were introduced by accounting for changes in CYP2D6 enzyme kinetics depending on activity score (AS), which in combination with AS for individual polymorphisms allowed us to model of CYP2D6 gene variants. Variability in CYP3A4 and CYP2D6 activity was modeled based on in vitro data from human liver microsomes. Model predictions are in very good agreement with pharmacokinetics data for CYP2D6 polymorphisms, CYP2D6 activity as measured by AS, and CYP2D6 metabolic phenotypes (UM, EM, IM, PM). The model was applied to investigate the genotype-phenotype association and the role of CYP2D6 polymorphisms for metabolic phenotyping with dextromethorphan using the urinary cumulative metabolic ratio DXM/(DXO+DXO-Glu) (UCMR). The effect of parameters on UCMR was studied via sensitivity analysis. Model predictions indicate very good robustness against the intervention protocol (i.e. application form, dosing amount, dissolution rate, and sampling time) and good robustness against physiological variation. The model is capable of estimating the UCMR dispersion within and across populations depending on activity scores. Moreover, the distribution of UCMR and the risk of genotype-phenotype mismatch could be estimated for populations with known CYP2D6 genotype frequencies. The model can be applied as a tool for individual prediction of UCMR and metabolic phenotype based on CYP2D6 genotype. Both, model and database are freely available for reuse.

Keywords: Dextromethorphan, CYP2D6, Physiologically based pharmacokinetic model, PBPK, Pharmacokinetics, Pharmacogenomics

1 INTRODUCTION

The cytochrome P450 (CYPs) superfamily of enzymes has a central role in the clearance of many substances and drugs, with the isoform 2D6 (CYP2D6) being one of the most important xenobiotic-metabolizing enzymes. CYP2D6 is involved in the clearance of around 20% of the most prescribed drugs (Saravanakumar et al., 2019) including antiarrhythmics (e.g. flecainide, procainamide, mexiletine), anticancer agents (e.g. tamoxifen), antidepressants (e.g. citalopram, fluoxetine, duloxetine: venlafaxine), antipsychotics (e.g. aripiprazole, haloperidol, thioridazine), β -blockers (metoprolol), analgesics (tramadol, oxycodone, codeine), and antitussives (dextromethorphan) (Kibaly et al., 2021; Hurtado et al., 2020). CYP2D6-mediated drug response exhibits a particularly large inter-individual variability which poses a challenge for personalized dosage of medication. The activity of CYP2D6 is known to be majorly dependent on genetic variants (Preskorn et al., 2013; Berm et al., 2013; Shah and Smith, 2015) with polymorphism of CYP2D6 being related to the risk of adverse effects, non-response during treatment, and death by drug intoxication (Gasche et al., 2004; Kawanishi et al., 2004; Rau et al., 2004; Zackrisson et al., 2010).

In the late 70s, a polymorphism in debrisoquine hydroxylation (Mahgoub et al., 1977) and sparteine oxidation (Eichelbaum et al., 1979) was discovered and subsequently attributed to allelic variants of the CYP2D6 gene. In the following years, CYP2D6 became one of the most studied drug-metabolizing enzymes. Genetic variants were classified into distinct phenotypes and subjects carrying combinations of these variants were categorized as poor metabolizer (gPM), intermediate metabolizer (gIM), extensive metabolizer (gEM), and ultra rapid metabolizer (gUM) (Zanger et al., 2004; Gaedigk et al., 2017). This classification is based on the relationship between genetic variants and CYP2D6-mediated drug response. For these genetically predicted phenotypes, we use the 'g' nomenclature as they can easily be confused with the actual *in vivo* metabolic phenotype, determined based on pharmacokinetic measurements after the administration of CYP2D6 test drugs. Nowadays, the CYP2D6 activity score (AS) system, a more refined metric, is often applied to characterize genotype-phenotype associations (Gaedigk et al., 2018a). In the system, discrete values between 0 and 1 are assigned to gene variants. The final activity score is calculated by addition of the activity scores of both alleles. For instance, for a person with diplotype *1/*3, the variant *1 has an AS of 1, and the variant *3 has no activity with an AS of 0, resulting in an overall AS of 1. Higher activity scores than 2 and additional complexity arise from copy number variation (CNV), chimeras, and hybrids with the pseudo gene CYP2D7. This can result in ambiguities and difficulties in the assignment of the correct diplotype and activity score (Gaedigk et al., 2007; Nofziger and Paulmichl, 2018; Gaedigk et al., 2019). Of note, AS specifics are still under heavy debate and regularly updated (Caudle et al., 2020). A multitude of population studies have been conducted to identify and associate allele variants with metabolic phenotypes within and across populations (Gaedigk et al., 2017). Over 130 CYP2D6 star (*) allele haplotypes have been identified and subsequently cataloged by the Pharmacogene Variation (PharmVar) Consortium into PharmGKB with their respective activity score contribution (Gaedigk et al., 2018b; Whirl-Carrillo et al., 2021).

Various methods exist for the metabolic phenotyping based on test substances. The gold standard is plasma concentration sampling of probe substances and their metabolites at various time points after the administration. (Partial) clearance rates and thereby the relative enzyme activities can be calculated from these plasma time profiles. Simplified methods have been established for many probe substances, e.g., the (cumulative) metabolic ratios between the probe substance and one or several of its metabolites at a single time point in blood, plasma, or urine are utilized as such proxy measures. Large-scale population studies often tend to employ urinary ratios of metabolites. Although, alternatives in saliva and breath are worth considering (De Kesel et al., 2016). Probe substances for metabolic phenotyping of CYP2D6 are

72 debrisoquine, dextromethorphan, metoprolol, or sparteine (Frank et al., 2007; Fuhr et al., 2007). Bufuralol
73 is less popular but well suited for *in vitro* investigations due to its fluorescent properties (Zanger et al.,
74 2004). Although debrisoquine and sparteine have excellent properties for CYP2D6 phenotyping, they
75 have been withdrawn from clinical use in most countries and are therefore no longer readily available.
76 Frequently in use for the phenotyping of CYP2D6 activity are metoprolol and dextromethorphan.

77 Dextromethorphan (DXM) is an over-the-counter, antitussive, non-narcotic, synthetic analog of codeine
78 affecting the activity of numerous channels and receptors in the brain that trigger the cough reflex (Silva
79 and Dinis-Oliveira, 2020). It is generally well-tolerated, considered safe in therapeutic dosage, and easily
80 available (Fuhr et al., 2007). Besides therapeutic purposes, DXM is most commonly applied as a probe
81 substance for CY2D6 phenotyping, alone or with other probe substances in a cocktail. DXM can be
82 administered orally and intravenously, has low bioavailability ($\approx 50\%$) and a rapid first-pass effect in the
83 intestine and liver. Typically only about half of the dose is recovered in urine over at least 12 hours after
84 administration, primarily as glucuronides (Schadel et al., 1995; Capon et al., 1996; Tenneze et al., 1999;
85 Strauch et al., 2009). In the systemic circulation, $\approx 55\text{--}65\%$ of DXM is non-specifically bound to plasma
86 proteins (Lutz and Isoherranen, 2012; Taylor et al., 2016).

87 The biotransformation of DXM is mostly confined to the liver, where DXM is O-demethylated by
88 CYP2D6 to the active metabolite dextrorphan (DXO). Subsequently to O-demethylation, most of the
89 DXO is rapidly transformed via UDP-glucuronosyltransferase (UGT) to dextrorphan O-glucuronide
90 (DXO-Glu) and excreted via the urine. In individuals without any functional variant of CYP2D6, the
91 metabolism of DXM to DXO is extremely slow but still present. Apparently, the O-demethylation
92 is not exclusively mediated by CYP2D6. Inhibition of CYP2D6, e.g., barely affects PMs (Pope et al.,
93 2004). Further, it has been shown *in vitro* that O-demethylation is secondary mediated also by CYP3A4,
94 CYP3A5 and CYP2C9 (von Moltke et al., 1998; McGinnity et al., 2000; Takashima et al., 2005; Yu
95 and Haining, 2001). The second pathway for DXM goes via N-demethylation to 3-methoxymorphinan
96 which is mainly catalyzed via CYP3A4. Subsequently, 3-methoxymorphinan and DXO are biotransformed
97 to 3-hydroxymorphinan which is then rapidly transformed via glucuronidation to hydroxymorphinan O-
98 glucuronide and excreted in the urine. The urinary cumulative metabolic ratio (UCMR) of DXM to its
99 metabolites DXM/(DXO+DXO-Glu) is a widely applied measure for the *in vivo* CYP2D6 phenotyping.

100 An crucial question for metabolic phenotyping and liver function testing is how CYP2D6 polymorphisms
101 affect the pharmacokinetics of DXM and metabolic phenotyping based on DXM, such as the UCMR. The
102 objective of this work was to answer this question by the means of physiologically based pharmacokinetic
103 (PBPK) modeling of DXM.

2 MATERIAL AND METHODS

104 2.1 Pharmacokinetics database of DXM

105 Pharmacokinetics data of DXM was systematically curated from literature for model development,
106 parameterization, and validation. Curation efforts were mainly focused on concentration-time profiles
107 of DXM, DXO, and DXO-Glu in plasma or serum and their amounts or ratios in urine. The data is
108 accompanied by metadata on the investigated subjects and groups (e.g. CYP2D6 genotype or activity
109 score) and the applied intervention (e.g. dose and application form of DXM). All data was curated using
110 an established curation pipeline (Grzegorzewski et al., 2022) and is available via the pharmacokinetics
111 database PK-DB (<https://pk-db.com>) (Grzegorzewski et al., 2021). As a first step, a PubMed search
112 for the pharmacokinetics of dextromethorphan in combination with genotyping and/or phenotyping was

113 performed with the search query <https://pubmed.ncbi.nlm.nih.gov/?term=dextromethorphan+AND+%28phenotype+OR+phenotyping%29+AND+genotype>. The literature corpus
114 was extended with drug cocktail studies from PK-DB (Grzegorzewski et al., 2022), secondary literature
115 from references, and results from PKPDAI with the search query <https://app.pkpdai.com/?term=dextromethorphan> [REF]. Data was selected and curated based on eligibility criteria, see below.
116 During the curation process, the initial corpus was updated by additional publications from the references
117 and citations. A subset of the studies only reported pharmacokinetic parameters but not timecourses. These
118 studies were curated but were not used in the presented analyses.
119

121 To be eligible, studies had to report *in vivo* pharmacokinetics data for adult (age ≥ 18) humans after
122 administration of DXM or DXM hydrobromide. The application route of DXM was restricted to oral (PO)
123 or intravenous (IV). All application forms (e.g. tablet, capsule, solution) were accepted. No restrictions
124 were imposed on the dosing amount of DXM or coadministrations of other substances. Studies containing
125 coadministrations that affect the pharmacokinetics of DXM were identified during the modeling process
126 and excluded. The relevant outcome measures are concentration-time profiles in plasma, serum, and urine
127 amounts of DXM, DXM metabolites, or metabolic ratios of metabolites such as UCMR. Studies containing
128 pharmacokinetic parameters of DXM and its metabolites (e.g. clearance, half-life, AUC) and (urinary
129 cumulative) metabolic ratios of DXM and its metabolites were included. Data containing timecourses
130 and CYP2D6 genotype information were prioritized. Non-healthy subjects were excluded if the disease is
131 known to affect the pharmacokinetics of DXM or DXM metabolites. Study B from the PhD thesis of Frank
132 (2009) highly deviates from the remaining data and was therefore excluded. Further, Wyen et al. (2008)
133 was identified as a duplicate of Study E from the PhD thesis of Frank (2009) and excluded. The final set of
134 curated studies used in the presented analyses is provided in Tab. 1.

135 For the selection and evaluation of studies from the literature, the PRISMA-ScR guidelines were adopted
136 where applicable (Tricco et al., 2018). The initial corpus contained 404 studies. After screening, application
137 of eligibility criteria, and prioritization, a total of 47 studies were curated (see supplementary Fig. S1). Of
138 these studies, 36 contained data used in the present work (Tab. 1).

139 2.2 PBPK model of DXM

140 The PBPK model of DXM, DXO, and DXO-Glu (Fig. 1) was encoded in the Systems Biology
141 Markup Language (SBML) (Hucka et al., 2019; Keating et al., 2020). For development and visualization
142 sbmlutils (König, 2021b) and cy3sbml (König and Rodriguez, 2019) were used. The model is an ordinary
143 differential equation (ODE) model and numerical simulations were performed using sbmlsim (König,
144 2021a) based on the high-performance SBML simulator libroadrunner (Somogyi et al., 2015). The model
145 is available in SBML under CC-BY 4.0 license from <https://github.com/mattiaskoenig/dextromethorphan-model>. Within this work, version 0.9.0 of the model was used Grzegorzewski and König (2022).

147 The model is hierarchically organized. The top layer represents the whole body with organs and tissues
148 connected via the blood flow. Tissues with minor influence on the pharmacokinetics of DXM, DXO, or
149 DXO-Glu were lumped into the 'rest' compartment. Intravenous and oral application of DXM appears
150 in the venous and intestinal compartments, respectively. For the oral application of DXM, the fraction
151 absorbed determines the DXM fraction which enters the systemic circulation via absorption and the fraction
152 excreted via the feces. The plasma concentration in the model is evaluated at the median cubital vein.

153 The distribution of DXM, DXO, and DXO-Glu between plasma and tissue compartments is based on
154 tissue-to-plasma partition coefficients (K_p) and corresponding rates of tissue distribution (f_{tissue}).

155 The metabolism of DXM only includes processes relevant for the simulation of the reported
156 pharmacokinetics data (see Fig. 1B and C). Routes of minor contribution such as N-demethylation of DXM
157 in the liver were neglected. Metabolic reactions take place in the intestine and liver and are modeled using
158 irreversible Michaelis-Menten reaction kinetics of the form $v = V_{max} \cdot \frac{S}{S+K_m}$, with V_{max} and K_m for
159 CYP3A4 and CYP2D6 sampled from distributions as described below. The conversion of DXM to DXO
160 can be either catalyzed via CYP2D6 (main route) or CYP3A4 (minor route) in the liver. Reactions with
161 other products than DXM, DXO, and DXO-Glu were modeled as annihilations, i.e., the products of the
162 reactions are not modeled explicitly. DXM, DXO, and DXO-Glu are eliminated into the urine via renal
163 excretion.

164 A subset of model parameters were fitted by minimizing the distance between model predictions and data
165 using subsets of the data presented in Fig. 4, Fig. 5, Fig. 6, Fig. 7, Fig. 8, and Fig. 9.

166 2.3 CYP3A4 and CYP2D6

167 CYP2D6 and CYP3A4 variability was modeled via correlated bivariate lognormal distributions fitted
168 to *in vitro* data for CYP2D6 (Yang et al., 2012; Storelli et al., 2019a) and CYP3A4 (Yang et al., 2012),
169 respectively. The data was log10 transformed and a Gaussian, parameterized by the mean (μ) and standard
170 deviation, was fitted by maximum likelihood estimation. The multivariate distribution was realized by a
171 Gaussian copula which in turn was parameterized by Kendall's tau correlation coefficient from the data
172 (see Fig. 2 for data and model).

173 In order to model the effect of the CYP2D6 activity score on activity, V_{max} was assumed to be proportional
174 to the activity score (AS), $V_{max} \propto AS$ and K_m was scaled by the activity score along the first principle
175 component of $\log_{10}(K_m)$ and $\log_{10}(V_{max})$. To model the effect of genetic polymorphisms of CYP2D6,
176 pharmacogenetic variants in the CYP2D6 gene were mapped to their activity score and the total activity
177 calculated as the sum of the activity of the two alleles. The genotype-phenotype definitions (i.e. allele
178 variant to activity score mapping) were used from PharmGKB (Whirl-Carrillo et al., 2021) (Tab. S1).

179 The stochastic model of CYP2D6 kinetics for a given population consists of a mixture model
180 comprised from the models for each activity score weighted by their respective frequency $P(AS)$, i.e.,
181 $P(V_{max}, K_m) = \sum_{AS} P(AS)P(V_{max}, K_m | AS)$. To simulate a given activity score, the respective K_m and
182 V_{max} values were used (see Fig. 2). The variability in pharmacokinetics was simulated by sampling
183 K_m and V_{max} from the CYP3A4 and CYP2D6 distributions. Distributions of CYP3A4 and CYP2D6
184 parameters were assumed to be statistically independent. To simulate different populations, the activity
185 score frequencies for the respective biogeographical population from PharmGKB (Whirl-Carrillo et al.,
186 2021) were used (Tab. S2).

187 2.4 CYP2D6 metabolic phenotype

188 The metabolic phenotypes ultrarapid metabolizer (UM), extensive metabolizer (EM), intermediate
189 metabolizer (IM), and poor metabolizer (PM) were assigned based on the urinary cumulative metabolic ratio
190 of DXM to total dextrorphan UCMR = $\frac{DXM}{DXO+DXO-Glu}$ with the following cutoffs: PM: UCMR ≥ 0.3 ,
191 IM: $0.03 \leq UCMR < 0.3$, EM: $0.0003 \leq UCMR < 0.03$, UM: UCMR < 0.0003 . Some studies reported
192 the extensive metabolizer as normal metabolizer (NM) with identical cutoffs to the EM.

193 2.5 Sensitivity analysis

194 A local sensitivity analysis of the effect of model parameters on the UCMR was performed.
195 Individual model parameters (p_i) were varied in both direction by 10% from the base model value

196 ($p_{i,-\Delta} \xleftarrow{10\%} p_{i,0} \xrightarrow{10\%} p_{i,\Delta}$) and the change in the state variable describing the UCMR at 8hr (q) was
197 recorded. The local sensitivity ($S(q, p_i, AS)$) was calculated for a range of activity scores ($AS = 0, 0.25,$
198 $0.5, 1, 1.25, 1.5, 2.0, 3.0$) by the following formula:

$$S(q, p_i, AS) = \frac{1}{2} \cdot \frac{q(p_{i,\Delta}, AS) - q(p_{i,-\Delta}, AS)}{p_{i,0}} \quad (1)$$

3 RESULTS

199 Within this work, a physiologically based pharmacokinetic (PBPK) model of DXM was developed and
200 applied to study the role of the CYP2D6 polymorphism on the pharmacokinetics of DXM and metabolic
201 phenotyping using DXM.

202 3.1 Pharmacokinetics database of DXM

203 For the development and evaluation of the model, a large pharmacokinetics dataset of DXM and its
204 metabolites, consisting of 36 clinical studies, was established (Tab. 1). Most of the studies investigated either
205 drug-gene (DGI), drug-drug interactions (DDI), or the interplay of both (i.e. drug-drug-gene interactions).
206 The large majority of studies applied DXM orally (n=35), whereas only a single publication Duedahl
207 et al. (2005) studied DXM pharmacokinetics after intravenous application (n=1). The application form (i.e.
208 solution, syrup, capsule, table), the used DXM dose (2 mg to 3 mg/kg), coadministrations (i.e. phenotyping
209 cocktail, quinidine, cinacalcet hydrochloride, zuojin) vary between studies, as do sampling times and
210 sampled tissues (i.e. urine, plasma, serum). Importantly, plenty of individual UCMR measurements with
211 corresponding CYP2D6 genotype information were contained within the dataset (n=11 studies). To our
212 knowledge, this is the first large freely available dataset of pharmacokinetics data for DXM with all data
213 accessible from the pharmacokinetics database (PK-DB) (Grzegorzewski et al., 2021).

214 3.2 PBPK model of DXM

215 Within this work, a PBPK model was developed (Fig. 1) to study the role of CYP2D6 polymorphism on
216 DXM pharmacokinetics and metabolic phenotyping with DXM. Important model parameters are provided
217 in Tab. 2. The model is organized hierarchically, with the top layer representing the whole body (Fig. 1A)
218 consisting of the liver, kidney, intestine, forearm, lung, and the rest compartment. Organs with minor
219 relevance are not modeled explicitly and lumped into the rest compartment. Organs are coupled via the
220 systemic circulation with the arrow width proportional to relative blood flow. DXM can be administered
221 intravenously (IV) or orally (PO) with DXM appearing in the venous blood or intestine, respectively.
222 The intestinal model (Fig 1B) describes dissolution, absorption and excretion of DXM. Only a fraction
223 of DXM is absorbed, with the remainder excreted in the feces. DXM enters the circulatory system by
224 crossing the enterocytes of the intestinal wall. First pass metabolism of DXM via CYP3A4 N-demethylation
225 in the intestine reduces the amount of DXM appearing in the systemic circulation. In the liver model
226 (Fig 1C), DXM gets transformed via O-demethylation to DXO and subsequently transformed to DXO-Glu.
227 The reactions are modeled by Michaelis-Menten kinetics and characterized with K_m and V_{max} values.
228 O-demethylation takes place via CYP3A4 and CYP2D6. The K_m and V_{max} of CYP2D6 is modulated via
229 the activity score, details can be found in section 3.3. The kidney model (Fig 1D) describes the urinary
230 excretion of DXM, DXO, and DXO-Glu.

231 The model allows to predict concentrations and amounts of DXM, DXO, and DXO-Glu depending on
232 CYP2D6 polymorphism, CYP2D6 diplotype, and CYP2D6 activity score with amounts and concentrations
233 of DXM, DXO, and DXO-Glu being evaluated in urine or the median cubital vein (plasma).

234 To our knowledge, this is the first freely accessible, reproducible, and reusable PBPK model of DXM
235 with the model available in SBML from <https://github.com/matthiaskoenig/dextromethorphan-model>.

236 **3.3 CYP3A4 and CYP2D6 variability**

237 Cytochrome P450 enzymes exhibit enormous inter-individual variability in enzyme activity. To
238 account for this variability a stochastic model of CYP2D6 and CYP3A4 activity based on bivariate
239 lognormal distributions of K_m and V_{max} was developed and fitted to experimental data from human liver
240 microsomes (Storelli et al., 2019a; Yang et al., 2012) (see Fig. 2).

241 For the CYP2D6 model, the V_{max} is assumed to be linearly related to the activity score with $AS = 0$
242 having no CYP2D6 activity. The dispersion of K_m and V_{max} are assumed to be constant for all activity
243 scores. For the mixture model, the frequencies of the individual activity scores $P(AS)$ are adopted from our
244 curated dataset (i.e., relative amount of subjects with reported activity scores and UCMRs). With increasing
245 activity score the maximal reaction velocity V_{max} of DXM conversion via CYP2D6 increases as does
246 the affinity for the substrate DXM (K_m decreases). The models of CYP3A4 and CYP2D6 are capable
247 of reproducing the data from the literature, but limited information on CYP2D6 genetics within the data
248 hinders the validation of the AS-specific model.

249 As motivated in the introduction, even subjects carrying no functional variant of the CYP2D6 gene
250 do metabolize DXM to DXO, however extremely slowly. This was implemented in the model via a
251 secondary O-demethylation via CYP3A4 with mean K_m for DXM adopted from Yu and Haining (2001).
252 The dispersion of K_m and V_{max} is assumed to be identical to the one measured by midazolam in Storelli
253 et al. (2019a) and Yang et al. (2012).

254 The resulting CYP3A4 and CYP2D6 enzyme model was coupled to the PBPK model and allowed to
255 account (i) for the variability in DXM pharmacokinetics due to the variability in CYPs parameters and (ii)
256 the effect of the activity score on CYP2D6 activity and consequently DXM pharmacokinetics.

257 **3.4 Effect of CYP2D6 activity score on DXM pharmacokinetics**

258 Model performance was visually assessed for common pharmacokinetic measurements (i.e., DXM, DXO,
259 and DXM/DXO in plasma and DXM/(DXO+DXO-Glu) in urine) and for subjects with reported AS or
260 diplotype (Fig. 3). For each activity score, a virtual population based on 2000 K_m and V_{max} samples was
261 created from the stochastic models of CYP3A4 and CYP2D6 model. For each set of samples the PBPK
262 model was simulated with an oral application of 30mg DXM and compared to the reported data. The
263 model predicts large relative variance within a AS group and across AS groups. With increasing AS and
264 consequently CYP2D6 activity, plasma DXM decreases (Fig. 3A), plasma DXO increases (Fig. 3B) and
265 the plasma DXM/DXO decreases (Fig. 3C) in very good agreement with the data (Chen et al., 2017; Frank,
266 2009). The large variability within a AS group is a consequence of the large variability of K_m and V_{max} in
267 the AS model of CYP2D6 (see Fig. 2). Due to the large overlap between distributions of neighboring AS,
268 also the pharmacokinetics timecourses show a large overlap between neighboring AS.

269 The UCMR (Fig. 3D) is very stable over time with good agreement with the data. With increasing activity
270 score, the UCMR decreases resulting in a shift from PM to EM metabolic phenotype. In the figure, UCMR

271 data independent of the applied DXM dose was pooled (in contrast to A-C only using 30mg data) and
272 compared to the simulation as the UCMR endpoint is very robust against the given dose (see section 3.5).

273 Overall the model predictions of DXM pharmacokinetics depending on AS are in very good agreement
274 with the available data despite the limited availability of pharmacokinetics timecourses for the low AS 0,
275 0.25, and 0.5.

276 To further evaluate the model performance, simulations were compared to pharmacokinetics data for
277 DXM in plasma or serum (Fig. 4), DXO in plasma or serum (Fig. 5), and DXO+DXO-Glu in plasma
278 or serum (Fig. 6), DXM in urine (Fig. 7), DXO+DXO-Glu in urine (Fig. 8), and the UCMR (Fig. 9).
279 With expected variability in mind, the model is capable to reproduce all data from the pharmacokinetics
280 dataset. Minor shortcomings of the model are faster kinetics of DXO+DXO-Glu in plasma (Fig. 6), which
281 is probably due to non-individual tissue-to-plasma coefficients for the respective tissues in the model. We
282 decided a for a more parsimonious model.

283 3.5 Effect of parameters on metabolic phenotyping via UCMR

284 Analysis of the effect of parameter changes on UCMR is highly relevant as it can help to identify potential
285 confounding factors and bias in UCMR based phenotyping. Of special importance for CYP2D6 is the
286 question if there is a dependency on the genetic polymorphism (activity score) of these effects.

287 To answer this question, model parameters (i.e., liver volume, cardiac output, tissue-to-plasma partition
288 coefficient of DXM, and oral dose) were changed in reasonable ranges and the effect on UCMR at 8hr after
289 the application of 30 mg of DXM was investigated (Fig. 10A). Independent of the AS, UCMR increased
290 with increasing liver volume and decreased with increasing cardiac output. A change in the tissue-to-plasma
291 partition coefficient of DXM or the amount of oral DXM barely affected UCMR.

292 CYP2D6 phenotyping by UCMR is very stable over time as demonstrated in the time course predictions
293 (see 3D and Fig. 9) and robust against changes in factors related to the intervention protocol (i.e. dosing
294 amount of DXM, dissolution rate) and to some extent against changes in physiological parameters (see
295 local sensitivity analysis of UCMR in Fig. 10B).

296 Liver volume, heart rate, cardiac output, kidney volume, and kidney elimination rate of DXM altered the
297 UCMR with a similar magnitude as the CYP2D6 reaction parameters. However, the biological variation
298 in these physiological parameters is orders of magnitude lower. The sensitivity analysis showed no effect
299 of UGT V_{max} and K_m on UCMR which is the reason why inter-individual variability of UGT activity
300 was not further investigated in this work. Local sensitivity of UCMR was almost identical at different AS
301 values for almost all parameters, i.e., the effect of physiological parameters is of similar relative magnitude
302 independent of activity score. For AS=0, our model assumptions of minor DXM metabolism by CYP3A4
303 lead to UCMR not being modulated by CYP2D6 but rather by CYP3A4 activity. Nonetheless, even across
304 studies with non-standardized intervention protocols the UCMR measurements seams to be a good but not
305 perfect endpoint to quantify and compare CYP2D6 enzyme activity. Importantly, our analysis indicates
306 that UCMR measurements can be pooled even across investigations with different intervention protocols.
307 This still may lead to biases and errors, e.g. due to differences in the quantification protocol.

308 3.6 Effect of CYP2D6 polymorphisms and activity score on UCMR

309 Next, we tested if the model is able to predict UCMR distributions for given genotypes and AS (Fig. 11).
310 Model predictions based on underlying genotype frequencies were compared with the experimental data.
311 UCMR distributions for individual AS groups are well described by the model. The AS impacts the

312 UCMR, with increasing AS resulting in an decrease in UCMR. However individual AS distributions
313 heavily overlap, as expected, due to the large overlap in CYP2D6 parameter distributions between different
314 AS. The predicted distributions tend to be slightly narrower than the actual data. Possible reasons are many
315 fold (e.g. omitted physiological variation, omitted variation in UGT activity, difficulties in correct genotype
316 assignment, unknown effect modifiers, and biases).

317 The AS system could be refined to better describe the data. The categorization of CYP2D6 genotypes
318 into discrete activity values (i. e. 0, 0.25, 0.5, 1) is an oversimplification, a continuous activity score
319 would probably perform better. The model and data indicate that gUM ($AS \geq 3$) is a very unreliable
320 predictor for ultra rapid metabolism and only gPMs ($AS = 0$) are almost perfectly distinguishable from
321 other metabolizers, see Fig. 11C, D, E, and F.

322 A strength of the presented model is that it enables the prediction of the *in vivo* phenotype of subjects
323 based on *in vitro* data.

324 3.7 Population variability in UCMR

325 Finally, the model was also capable to predict UCMR distributions for different biogeographical
326 populations (Fig. 12) based on the underlying AS frequencies (Tab. S2). Based on the reported frequencies,
327 the UCMR distributions were simulated at 8hr after the application of 30mg DXM for Oceanian, Near
328 Eastern, American, Latino, Central/South Asian, African American/Afro-Caribbean, Sub-Saharan African,
329 European, and East Asian populations (Fig. 12A). Data for Caucasian and East Asian populations (Fig. 12B)
330 was used for validation of the predictions (Fig. 12C). The data is in good agreement with measurements
331 of Caucasians and East Asians as reported by Abdelrahman et al. (1999); Frank (2009); Gaedigk (2013);
332 Köhler et al. (1997); Myrand et al. (2008).

4 DISCUSSION

333 During the last 20 years various modeling approaches and software solutions were utilized to
334 investigate various aspects of DXM pharmacokinetics, e.g. using GastroPlus (Bolger et al., 2019), P-
335 Pharm (Moghadamnia et al., 2003), SAS (Ito et al., 2010; Chiba et al., 2012), SimCYP (Dickinson et al.,
336 2007; Ke et al., 2013; Sager et al., 2014; Chen et al., 2016; Rougée et al., 2016; Adiwidjaja et al., 2018;
337 Machavaram et al., 2019; Storelli et al., 2019b), MATLAB (Kim et al., 2017), or PK-Sim (Rüdesheim
338 et al., 2022). However, most of the work is difficult/impossible to validate or to build up on due to a lack
339 of accessibility of models and software, and platform-independence of the models. Here, we provide an
340 openly accessible, reproducible and platform-independent whole-body model of DXM metabolism, which
341 facilitates reusability, extensibility, and comparability.

342 Apart from that, modeling work which aims for high empirically evidence relies on trustworthy supporting
343 real world data. More and independent sources of data are highly beneficial for the scientific outcomes. For
344 that matter, guidelines like PRISMA for reporting transparency, completeness, and accuracy find very broad
345 endorsement in the field of systematic reviews and meta analysis. The present work faces somewhat similar
346 challenges for the evaluation and selection of data from literature. Therefore, PRISMA-ScR guidelines
347 were adopted where applicable. With this approach, bias within the used dataset could be mitigated or
348 at least identified. Importantly, we supplement our open and accessible model with a large, open, and
349 accessible database of pharmacokinetics data.

350 The presented PBPK model is able to predict the DXM metabolism of populations and individuals based
351 on their CYP2D6 genotype. It is probably the first model capable to predict individual UCMRs. Moreover,

352 it can reproduce a broad range of reported clinical data on DXM and enables better intuition on how to
353 interpret DXM related pharmacokinetics. E.g., CYP2D6 activity is not the only modulator of UCMR, as
354 can be seen by the large variability in activity score and overlap between activity scores. UCMR as a proxy
355 of CYP2D6 metabolic phenotype should therefore be interpreted carefully. The model shows e.g. that for
356 extremely low CYP2D6 activity the UCMR is not primarily governed by the CYP2D6 activity. This is
357 consistent with the finding that CYP2D6 inhibition merely affects PMs (Pope et al., 2004).

358 The current version of the model is already very valuable, still there is plenty of room for improvement.
359 By providing the data and model in open and standardized formats we enable and encourage these
360 improvements by model extensions and updates.

361 Many of the physiological parameters in the model were fitted or estimated although they could be
362 measured in principle. E.g., relatively low DXM concentrations in plasma suggest substantial extra-
363 vascular binding of DXM. However, tissue-plasma partition coefficients (K_p) are difficult to assess and only
364 limited data is available. Steinberg et al. (1996) reported brain levels to be 68-fold higher and cerebrospinal
365 fluid levels 4-fold lower than serum levels, respectively. Others estimated $K_p \sim 1.65$ from n-octanol-
366 water partition coefficients and again others suggested additional trapping mechanisms (i.e., lysosomal
367 trapping) (Bolger et al., 2019). In the model, the DXO-Glu kinetics is a bit too fast (see Fig. 6), probably due
368 to the decision to use a single K_p and f_{tissue} parameter for all tissues for a given substance. Glucuronides,
369 however, are generally much more polar than their respective non-glucuronides which result in less plasma
370 binding, higher urinary excretion, lower lipid-solubility, and higher water-solubility. Transport into different
371 tissues is affected differently by polarity. Next, The impact of urinary excretion rates and the effect of
372 urinary pH is probably also important but data is very limited (Labbé et al., 2000; Özdemir et al., 2004;
373 Fuhr et al., 2007).

374 Most important for model improvements would be additional *in vitro* measurements on the association
375 between CYP2D6 genotype and phenotype which are very limited in literature (Storelli et al., 2019a;
376 Ning et al., 2019; Dalton et al., 2020) and simultaneous *in vitro* and UCMR measurements with no such
377 data available in the literature. Both would be very important for the validation of the AS system and the
378 development of new models which e.g. take into account structural variation (Dalton et al., 2020). For
379 instance, with the AS system alone it is not possible to explain why CYP2D6 is inhibited differently for
380 different genotypes Qiu et al. (2016).

381 In conclusion, we developed and validated a PBPK model of DXM and applied it to study the effect of
382 the CYP2D6 polymorphism on metabolic phenotyping.

CONFLICT OF INTEREST STATEMENT

383 All authors declare that the research was conducted in the absence of any commercial or financial
384 relationships that could be construed as a potential conflict of interest.

AUTHOR CONTRIBUTIONS

385 JG and MK designed the study, developed the computational model, implemented and performed the
386 analysis, and wrote the initial draft of the manuscript. JB provided support with data curation. All authors
387 discussed the results. All authors contributed to and revised the manuscript critically.

FUNDING

388 JG, JB and MK were supported by the Federal Ministry of Education and Research (BMBF, Germany)
389 within the research network Systems Medicine of the Liver (LiSyM, grant number 031L0054). MK
390 and JG were supported by the German Research Foundation (DFG) within the Research Unit Program
391 FOR 5151 "QualiPerF (Quantifying Liver Perfusion-Function Relationship in Complex Resection - A
392 Systems Medicine Approach)" by grant number 436883643 and MK by grant number 465194077 (Priority
393 Programme SPP 2311, Subproject SimLivA).

DATA AVAILABILITY STATEMENT

394 All clinical data of dextromethorphan pharmacokinetics that was used in this work can be found in PK-DB
395 available from <https://pk-db.com>.

REFERENCES

- 396 Abdelrahman, S., Gotschall, R., Kauffman, R., Leeder, J., and Kearns, G. (1999). Investigation of
397 terbinafine as a CYP2D6 inhibitor in vivo. *Clinical Pharmacology & Therapeutics* 65, 465–472.
398 doi:10.1016/S0009-9236(99)70065-2
- 399 Abduljalil, K., Frank, D., Gaedigk, A., Klaassen, T., Tomalik-Scharte, D., Jetter, A., et al. (2010).
400 Assessment of Activity Levels for CYP2D6*1, CYP2D6*2, and CYP2D6*41 Genes by Population
401 Pharmacokinetics of Dextromethorphan. *Clinical Pharmacology & Therapeutics* 88, 643–651. doi:10.1
402 038/clpt.2010.137
- 403 Adiwidjaja, J., Boddy, A. V., and McLachlan, A. J. (2018). A Strategy to Refine the Phenotyping Approach
404 and Its Implementation to Predict Drug Clearance: A Physiologically Based Pharmacokinetic Simulation
405 Study. *CPT: Pharmacometrics & Systems Pharmacology* 7, 798–808. doi:10.1002/psp4.12355
- 406 Armani, S., Ting, L., Sauter, N., Darstein, C., Tripathi, A. P., Wang, L., et al. (2017). Drug Interaction
407 Potential of Osilodrostat (LCI699) Based on Its Effect on the Pharmacokinetics of Probe Drugs of
408 Cytochrome P450 Enzymes in Healthy Adults. *Clinical drug investigation* 37, 465–472. doi:10.1007/s4
409 0261-017-0497-0
- 410 Barnhart, J. W. (1980). The urinary excretion of dextromethorphan and three metabolites in dogs and
411 humans. *Toxicology and Applied Pharmacology* 55, 43–48. doi:10.1016/0041-008X(80)90218-5
- 412 Berm, E. J. J., Risselada, A. J., Mulder, H., Hak, E., and Wilffert, B. (2013). Phenoconversion of
413 cytochrome P450 2D6: The need for identifying the intermediate metabolizer genotype. *The Journal of
414 clinical psychiatry* 74, 1025. doi:10.4088/JCP.13lr08555
- 415 Bolger, M. B., Macwan, J. S., Sarfraz, M., Almukainzi, M., and Löbenberg, R. (2019). The Irrelevance
416 of In Vitro Dissolution in Setting Product Specifications for Drugs Like Dextromethorphan That are
417 Subject to Lysosomal Trapping. *Journal of pharmaceutical sciences* 108, 268–278. doi:10.1016/j.xphs
418 .2018.09.036
- 419 Capon, D. A., Bochner, F., Kerry, N., Mikus, G., Danz, C., and Somogyi, A. A. (1996). The influence of
420 CYP2D6 polymorphism and quinidine on the disposition and antitussive effect of dextromethorphan in
421 humans*. *Clinical Pharmacology & Therapeutics* 60, 295–307. doi:10.1016/S0009-9236(96)90056-9
- 422 Caudle, K. E., Sangkuhl, K., Whirl-Carrillo, M., Swen, J. J., Haidar, C. E., Klein, T. E., et al. (2020).
423 Standardizing CYP 2D6 Genotype to Phenotype Translation: Consensus Recommendations from the
424 Clinical Pharmacogenetics Implementation Consortium and Dutch Pharmacogenetics Working Group.
425 *Clinical and Translational Science* 13, 116–124. doi:10.1111/cts.12692

- 426 Chen, R., Rostami-Hodjegan, A., Wang, H., Berk, D., Shi, J., and Hu, P. (2016). Application of a
427 physiologically based pharmacokinetic model for the evaluation of single-point plasma phenotyping
428 method of CYP2D6. *European journal of pharmaceutical sciences : official journal of the European
429 Federation for Pharmaceutical Sciences* 92, 131–136. doi:10.1016/j.ejps.2016.07.001
- 430 Chen, R., Zheng, X., and Hu, P. (2017). CYP2D6 Phenotyping Using Urine, Plasma, and Saliva Metabolic
431 Ratios to Assess the Impact of CYP2D6*10 on Interindividual Variation in a Chinese Population.
432 *Frontiers in Pharmacology* 8, 239. doi:10.3389/fphar.2017.00239
- 433 Chiba, K., Kato, M., Ito, T., Suwa, T., and Sugiyama, Y. (2012). Inter-individual variability of in
434 vivo CYP2D6 activity in different genotypes. *Drug metabolism and pharmacokinetics* 27, 405–413.
435 doi:10.2133/dmpk.dmpk-11-rg-078
- 436 Chládek, J., Zimová, G., Beránek, M., and Martíková, J. (2000). In-vivo indices of CYP2D6 activity:
437 Comparison of dextromethorphan metabolic ratios in 4-h urine and 3-h plasma. *European Journal of
438 Clinical Pharmacology* 56, 651–657. doi:10.1007/s002280000218
- 439 Dalton, R., Lee, S.-B., Claw, K. G., Prasad, B., Phillips, B. R., Shen, D. D., et al. (2020). Interrogation of
440 CYP2D6 Structural Variant Alleles Improves the Correlation Between CYP2D6 Genotype and CYP2D6-
441 Mediated Metabolic Activity. *Clinical and translational science* 13, 147–156. doi:10.1111/cts.1269
442 5
- 443 De Kesel, P. M. M., Lambert, W. E., and Stove, C. P. (2016). Alternative Sampling Strategies for
444 Cytochrome P450 Phenotyping. *Clinical Pharmacokinetics* 55, 169–184. doi:10.1007/s40262-015-030
445 6-y
- 446 de Simone, G., Devereux, R. B., Daniels, S. R., Mureddu, G., Roman, M. J., Kimball, T. R., et al. (1997).
447 Stroke volume and cardiac output in normotensive children and adults. Assessment of relations with
448 body size and impact of overweight. *Circulation* 95, 1837–1843. doi:10.1161/01.cir.95.7.1837
- 449 Demirbas, S., Reyderman, L., and Stavchansky, S. (1998). Bioavailability of dextromethorphan (as
450 dextrorphan) from sustained release formulations in the presence of guaifenesin in human volunteers.
451 *Biopharmaceutics & Drug Disposition* 19, 541–545. doi:10.1002/(SICI)1099-081X(1998110)19:8<541::
452 AID-BDD138>3.0.CO;2-8
- 453 Dickinson, G. L., Rezaee, S., Proctor, N. J., Lennard, M. S., Tucker, G. T., and Rostami-Hodjegan, A.
454 (2007). Incorporating In Vitro Information on Drug Metabolism Into Clinical Trial Simulations to Assess
455 the Effect of CYP2D6 Polymorphism on Pharmacokinetics and Pharmacodynamics: Dextromethorphan
456 as a Model Application. *The Journal of Clinical Pharmacology* 47, 175–186. doi:10.1177/0091270006
457 294279
- 458 Dorado, P., González, I., Naranjo, M. E. G., de Andrés, F., Peñas-Lledó, E. M., Calzadilla, L. R.,
459 et al. (2017). Lessons from Cuba for Global Precision Medicine: CYP2D6 Genotype Is Not a Robust
460 Predictor of CYP2D6 Ultrarapid Metabolism. *OMICS: A Journal of Integrative Biology* 21, 17–26.
461 doi:10.1089/omi.2016.0166
- 462 Doroshyenko, O., Rokitta, D., Zadoyan, G., Klement, S., Schläfke, S., Dienel, A., et al. (2013). Drug
463 cocktail interaction study on the effect of the orally administered lavender oil preparation silexan on
464 cytochrome P450 enzymes in healthy volunteers. *Drug Metab. Dispos.* 41, 987–993. doi:10.1124/dmd.
465 112.050203
- 466 Duedahl, T. H., Dirks, J., Petersen, K. B., Romsing, J., Larsen, N.-E., and Dahl, J. B. (2005). Intravenous
467 dextromethorphan to human volunteers: Relationship between pharmacokinetics and anti-hyperalgesic
468 effect. *Pain* 113, 360–368. doi:10.1016/j.pain.2004.11.015
- 469 Dumond, J. B., Vourvahis, M., Rezk, N. L., Patterson, K. B., Tien, H.-C., White, N., et al. (2010). A
470 Phenotype–Genotype Approach to Predicting CYP450 and P-Glycoprotein Drug Interactions With the

- 471 Mixed Inhibitor/Inducer Tipranavir/Ritonavir. *Clinical Pharmacology & Therapeutics* 87, 735–742.
472 doi:10.1038/clpt.2009.253
- 473 Edwards, J. E., Eliot, L., Parkinson, A., Karan, S., and MacConell, L. (2017). Assessment
474 of Pharmacokinetic Interactions Between Obeticholic Acid and Caffeine, Midazolam, Warfarin,
475 Dextromethorphan, Omeprazole, Rosuvastatin, and Digoxin in Phase 1 Studies in Healthy Subjects.
476 *Advances in Therapy* 34, 2120–2138. doi:10.1007/s12325-017-0601-0
- 477 Eichelbaum, M., Spannbrucker, N., Steincke, B., and Dengler, H. J. (1979). Defective N-oxidation of
478 sparteine in man: A new pharmacogenetic defect. *European journal of clinical pharmacology* 16,
479 183–187. doi:10.1007/BF00562059
- 480 Eichhold, T. H., Greenfield, L. J., Hoke, S. H., and Wehmeyer, K. R. (1997). Determination
481 of dextromethorphan and dextrorphan in human plasma by liquid chromatography/tandem mass
482 spectrometry. *Journal of Mass Spectrometry* 32, 1205–1211. doi:10.1002/(SICI)1096-9888(199711)32:
483 11<1205::AID-JMS579>3.0.CO;2-C
- 484 Eichhold, T. H., McCauley-Myers, D. L., Khambe, D. A., Thompson, G. A., and Hoke, S. H. (2007).
485 Simultaneous determination of dextromethorphan, dextrorphan, and guaifenesin in human plasma using
486 semi-automated liquid/liquid extraction and gradient liquid chromatography tandem mass spectrometry.
487 *Journal of Pharmaceutical and Biomedical Analysis* 43, 586–600. doi:10.1016/j.jpba.2006.07.018
- 488 Frank, D. (2009). *Evaluation of pharmacokinetic metrics for phenotyping of the human CYP2D6 enzyme
489 with dextromethorphan*. Ph.D. thesis, Rheinische Friedrich-Wilhelms-Universität Bonn
- 490 Frank, D., Jaehde, U., and Fuhr, U. (2007). Evaluation of probe drugs and pharmacokinetic metrics for
491 CYP2D6 phenotyping. *European Journal of Clinical Pharmacology* 63, 321–333. doi:10.1007/s00228
492 -006-0250-8
- 493 Fuhr, U., Jetter, A., and Kirchheimer, J. (2007). Appropriate phenotyping procedures for drug metabolizing
494 enzymes and transporters in humans and their simultaneous use in the "cocktail" approach. *Clinical
495 pharmacology and therapeutics* 81, 270–283. doi:10.1038/sj.clpt.6100050
- 496 Gaedigk, A. (2013). Complexities of CYP2D6 gene analysis and interpretation. *International Review of
497 Psychiatry* 25, 534–553. doi:10.3109/09540261.2013.825581
- 498 Gaedigk, A., Dinh, J., Jeong, H., Prasad, B., and Leeder, J. (2018a). Ten Years' Experience with the
499 CYP2D6 Activity Score: A Perspective on Future Investigations to Improve Clinical Predictions for
500 Precision Therapeutics. *Journal of Personalized Medicine* 8, 15. doi:10.3390/jpm8020015
- 501 Gaedigk, A., Eklund, J. D., Pearce, R. E., Leeder, J. S., Alander, S. W., Phillips, M. S., et al. (2007).
502 Identification and characterization of CYP2D6*56B, an allele associated with the poor metabolizer
503 phenotype. *Clinical pharmacology and therapeutics* 81, 817–820. doi:10.1038/sj.clpt.6100125
- 504 Gaedigk, A., Ingelman-Sundberg, M., Miller, N. A., Leeder, J. S., Whirl-Carrillo, M., Klein, T. E., et al.
505 (2018b). The pharmacogene variation (PharmVar) consortium: Incorporation of the human cytochrome
506 P450 (CYP) allele nomenclature database. *Clinical pharmacology and therapeutics* 103, 399–401.
507 doi:10.1002/cpt.910
- 508 Gaedigk, A., Sangkuhl, K., Whirl-Carrillo, M., Klein, T., and Leeder, J. S. (2017). Prediction of CYP2D6
509 phenotype from genotype across world populations. *Genetics in Medicine: Official Journal of the
510 American College of Medical Genetics* 19, 69–76. doi:10.1038/gim.2016.80
- 511 Gaedigk, A., Turner, A., Everts, R. E., Scott, S. A., Aggarwal, P., Broeckel, U., et al. (2019).
512 Characterization of Reference Materials for Genetic Testing of CYP2D6 Alleles. *The Journal of
513 Molecular Diagnostics* 21, 1034–1052. doi:10.1016/j.jmoldx.2019.06.007

- 514 Gasche, Y., Daali, Y., Fathi, M., Chiappe, A., Cottini, S., Dayer, P., et al. (2004). Codeine intoxication
515 associated with ultrarapid CYP2D6 metabolism. *The New England journal of medicine* 351, 2827–2831.
516 doi:10.1056/NEJMoa041888
- 517 Grzegorzewski, J., Bartsch, F., Kölle, A., and König, M. (2022). Pharmacokinetics of Caffeine: A
518 Systematic Analysis of Reported Data for Application in Metabolic Phenotyping and Liver Function
519 Testing. *Frontiers in Pharmacology* 12. doi:10.3389/fphar.2021.752826
- 520 Grzegorzewski, J., Brandhorst, J., Green, K., Eleftheriadou, D., Duport, Y., Barthorscht, F., et al. (2021).
521 PK-DB: Pharmacokinetics database for individualized and stratified computational modeling. *Nucleic
522 Acids Research* 49, D1358–D1364. doi:10.1093/nar/gkaa990
- 523 [Dataset] Grzegorzewski, J. and König, M. (2022). Physiologically based pharmacokinetic (PBPK) model
524 of dextromethorphan. doi:10.5281/zenodo.6976103
- 525 Herman, I. P. (2016). *Physics of the Human Body* (Springer)
- 526 Hou, Z.-Y., Pickle, L. W., Meyer, P. S., and Woosley, R. L. (1991). Salivary analysis for determination
527 of dextromethorphan metabolic phenotype. *Clinical Pharmacology and Therapeutics* 49, 410–419.
528 doi:10.1038/clpt.1991.48
- 529 Hu, L., Li, L., Yang, X., Liu, W., Yang, J., Jia, Y., et al. (2011). Floating matrix dosage form for
530 dextromethorphan hydrobromide based on gas forming technique: In vitro and in vivo evaluation in
531 healthy volunteers. *European Journal of Pharmaceutical Sciences* 42, 99–105. doi:10.1016/j.ejps.2010.
532 10.010
- 533 Hucka, M., Bergmann, F. T., Chaouiya, C., Dräger, A., Hoops, S., Keating, S. M., et al. (2019). The
534 systems biology markup language (SBML): Language specification for level 3 version 2 core release 2.
535 *Journal of Integrative Bioinformatics* doi:10.1515/jib-2019-0021
- 536 Hurtado, I., García-Sempere, A., Peiró, S., and Sanfélix-Gimeno, G. (2020). Increasing Trends in Opioid
537 Use From 2010 to 2018 in the Region of Valencia, Spain: A Real-World, Population-Based Study.
538 *Frontiers in Pharmacology* 11, 612556. doi:10.3389/fphar.2020.612556
- 539 ICRP (2002). Basic anatomical and physiological data for use in radiological protection: Reference values.
540 A report of age- and gender-related differences in the anatomical and physiological characteristics of
541 reference individuals. ICRP Publication 89. *Annals of the ICRP* 32, 5–265
- 542 Ito, T., Kato, M., Chiba, K., Okazaki, O., and Sugiyama, Y. (2010). Estimation of the interindividual
543 variability of cytochrome 2D6 activity from urinary metabolic ratios in the literature. *Drug Metabolism
544 and Pharmacokinetics* 25, 243–253. doi:10.2133/dmpk.25.243
- 545 Jones, D. R., Gorski, J. C., Haehner, B. D., O'Mara, E. M., and Hall, S. D. (1996). Determination
546 of cytochrome P450 3A4/5 activity in vivo with dextromethorphan N-demethylation. *Clinical
547 Pharmacology and Therapeutics* 60, 374–384. doi:10.1016/S0009-9236(96)90194-0
- 548 Jones, H. and Rowland-Yeo, K. (2013). Basic concepts in physiologically based pharmacokinetic modeling
549 in drug discovery and development. *CPT: pharmacometrics & systems pharmacology* 2, e63. doi:10.1
550 038/psp.2013.41
- 551 Kawanishi, C., Lundgren, S., Agren, H., and Bertilsson, L. (2004). Increased incidence of CYP2D6
552 gene duplication in patients with persistent mood disorders: Ultrarapid metabolism of antidepressants
553 as a cause of nonresponse. A pilot study. *European Journal of Clinical Pharmacology* 59, 803–807.
554 doi:10.1007/s00228-003-0701-4
- 555 Ke, A. B., Nallani, S. C., Zhao, P., Rostami-Hodjegan, A., Isoherranen, N., and Unadkat, J. D. (2013).
556 A Physiologically Based Pharmacokinetic Model to Predict Disposition of CYP2D6 and CYP1A2
557 Metabolized Drugs in Pregnant Women. *Drug Metabolism and Disposition* 41, 801–813. doi:10.1124/
558 dmd.112.050161

- 559 Keating, S. M., Waltemath, D., König, M., Zhang, F., Dräger, A., Chaouiya, C., et al. (2020). SBML Level
560 3: An extensible format for the exchange and reuse of biological models. *Molecular systems biology* 16,
561 e9110. doi:10.15252/msb.20199110
- 562 Kerry, N., Somogyi, A., Bochner, F., and Mikus, G. (1994). The role of CYP2D6 in primary and secondary
563 oxidative metabolism of dextromethorphan: In vitro studies using human liver microsomes. *British
564 Journal of Clinical Pharmacology* 38, 243–248. doi:10.1111/j.1365-2125.1994.tb04348.x
- 565 Kibaly, C., Alderete, J. A., Liu, S. H., Nasef, H. S., Law, P.-Y., Evans, C. J., et al. (2021). Oxycodone in the
566 Opioid Epidemic: High ‘Liking’, ‘Wanting’, and Abuse Liability. *Cellular and Molecular Neurobiology*
567 41, 899–926. doi:10.1007/s10571-020-01013-y
- 568 Kim, E.-Y., Shin, S.-G., and Shin, J.-G. (2017). Prediction and visualization of CYP2D6 genotype-
569 based phenotype using clustering algorithms. *Translational and Clinical Pharmacology* 25, 147–152.
570 doi:10.12793/tcp.2017.25.3.147
- 571 Köhler, D., Härtter, S., Fuchs, K., Sieghart, W., and Hiemke, C. (1997). CYP2D6 genotype and phenotyping
572 by determination of dextromethorphan and metabolites in serum of healthy controls and of patients under
573 psychotropic medication. *Pharmacogenetics* 7, 453–461. doi:10.1097/00008571-199712000-00003
- 574 [Dataset] König, M. (2021a). Matthiaskoenig/sbmlsim: 0.1.14 - SBML simulation made easy. Zenodo.
575 doi:10.5281/zenodo.5531088
- 576 [Dataset] König, M. (2021b). Sbmlutils: Python utilities for SBML. Zenodo. doi:10.5281/zenodo.55466
577 03;https://web.archive.org/web/20211107162358/https://zenodo.org/record/5546603
- 578 [Dataset] König, M. and Rodriguez, N. (2019). Matthiaskoenig/cy3sbml: Cy3sbml-v0.3.0 - SBML for
579 Cytoscape. Zenodo. doi:10.5281/zenodo.3451319;https://web.archive.org/web/20200213084214/https:
580 //zenodo.org/record/3451319
- 581 Labbé, L., Sirois, C., Pilote, S., Arseneault, M., Robitaille, N. M., Turgeon, J., et al. (2000). Effect of
582 gender, sex hormones, time variables and physiological urinary pH on apparent CYP2D6 activity as
583 assessed by metabolic ratios of marker substrates. *Pharmacogenetics* 10, 425–438. doi:10.1097/000085
584 71-200007000-00006
- 585 Lenuzza, N., Duval, X., Nicolas, G., Thévenot, E., Job, S., Videau, O., et al. (2016). Safety and
586 pharmacokinetics of the CIME combination of drugs and their metabolites after a single oral dosing
587 in healthy volunteers. *European journal of drug metabolism and pharmacokinetics* 41, 125–138.
588 doi:10.1007/s13318-014-0239-0
- 589 López, M., Guerrero, J., Jung-Cook, H., and Alonso, M. E. (2005). CYP2D6 genotype and phenotype
590 determination in a Mexican Mestizo population. *European Journal of Clinical Pharmacology* 61,
591 749–754. doi:10.1007/s00228-005-0038-2
- 592 Lutz, J. D. and Isoherranen, N. (2012). Prediction of Relative In Vivo Metabolite Exposure from In Vitro
593 Data Using Two Model Drugs: Dextromethorphan and Omeprazole. *Drug Metabolism and Disposition*
594 40, 159–168. doi:10.1124/dmd.111.042200
- 595 Machavaram, K. K., Endo-Tsukude, C., Terao, K., Gill, K. L., Hatley, O. J., Gardner, I., et al. (2019).
596 Simulating the Impact of Elevated Levels of Interleukin-6 on the Pharmacokinetics of Various CYP450
597 Substrates in Patients with Neuromyelitis Optica or Neuromyelitis Optica Spectrum Disorders in
598 Different Ethnic Populations. *The AAPS journal* 21, 42. doi:10.1208/s12248-019-0309-y
- 599 Mahgoub, A., Idle, J. R., Dring, L. G., Lancaster, R., and Smith, R. L. (1977). Polymorphic hydroxylation
600 of Debrisoquine in man. *Lancet (London, England)* 2, 584–586. doi:10.1016/s0140-6736(77)91430-1
- 601 McGinnity, D. F., Parker, A. J., Soars, M., and Riley, R. J. (2000). Automated definition of the enzymology
602 of drug oxidation by the major human drug metabolizing cytochrome P450s. *Drug metabolism and
603 disposition: the biological fate of chemicals* 28, 1327–1334

- 604 Moghadamnia, A. A., Rostami-Hodjegan, A., Abdul-Manap, R., Wright, C. E., Morice, A. H., and Tucker,
605 G. T. (2003). Physiologically based modelling of inhibition of metabolism and assessment of the
606 relative potency of drug and metabolite: Dextromethorphan vs . dextrorphan using quinidine inhibition:
607 Dextromethorphan vs. dextrorphan using quinidine inhibition. *British Journal of Clinical Pharmacology*
608 56, 57–67. doi:10.1046/j.1365-2125.2003.01853.x
- 609 Montané Jaime, L. K., Lalla, A., Steimer, W., and Gaedigk, A. (2013). Characterization of the *CYP2D6*
610 gene locus and metabolic activity in Indo- and Afro-Trinidadians: Discovery of novel allelic variants.
611 *Pharmacogenomics* 14, 261–276. doi:10.2217/pgs.12.207
- 612 Myrand, S., Sekiguchi, K., Man, M., Lin, X., Tzeng, R.-Y., Teng, C.-H., et al. (2008).
613 Pharmacokinetics/Genotype Associations for Major Cytochrome P450 Enzymes in Native and First- and
614 Third-generation Japanese Populations: Comparison With Korean, Chinese, and Caucasian Populations.
615 *Clinical Pharmacology & Therapeutics* 84, 347–361. doi:10.1038/sj.clpt.6100482
- 616 Nagai, N., Kawakubo, T., Kaneko, F., Ishii, M., Shinohara, R., Saito, Y., et al. (1996).
617 PHARMACOKINETICS AND POLYMORPHIC OXIDATION OF DEXTROMETHORPHAN IN
618 A JAPANESE POPULATION. *Biopharmaceutics & Drug Disposition* 17, 421–433. doi:10.1002/(SICI)
619 1099-081X(199607)17:5<421::AID-BDD421>3.0.CO;2-9
- 620 Nakashima, D., Takama, H., Ogasawara, Y., Kawakami, T., Nishitoba, T., Hoshi, S., et al. (2007). Effect of
621 Cinacalcet Hydrochloride, a New Calcimimetic Agent, on the Pharmacokinetics of Dextromethorphan:
622 In Vitro and Clinical Studies. *The Journal of Clinical Pharmacology* 47, 1311–1319. doi:10.1177/0091
623 270007304103
- 624 Ning, M., Duarte, J. D., Stevison, F., Isoherranen, N., Rubin, L. H., and Jeong, H. (2019). Determinants
625 of Cytochrome P450 2D6 mRNA Levels in Healthy Human Liver Tissue. *Clinical and Translational*
626 *Science* 12, 416–423. doi:10.1111/cts.12632
- 627 Nofziger, C. and Paulmichl, M. (2018). Accurately genotyping *CYP2D6* : Not for the faint of heart.
628 *Pharmacogenomics* 19, 999–1002. doi:10.2217/pgs-2018-0105
- 629 Nyunt, M. M., Becker, S., MacFarland, R. T., Chee, P., Scarborough, R., Everts, S., et al. (2008).
630 Pharmacokinetic Effect of AMD070, an Oral CXCR4 Antagonist, on CYP3A4 and CYP2D6 Substrates
631 Midazolam and Dextromethorphan in Healthy Volunteers. *JAIDS Journal of Acquired Immune Deficiency*
632 *Syndromes* 47, 559–565. doi:10.1097/QAI.0b013e3181627566
- 633 Oh, K.-S., Park, S.-J., Shinde, D. D., Shin, J.-G., and Kim, D.-H. (2012). High-sensitivity liquid
634 chromatography-tandem mass spectrometry for the simultaneous determination of five drugs and their
635 cytochrome P450-specific probe metabolites in human plasma. *Journal of chromatography. B, Analytical*
636 *technologies in the biomedical and life sciences* 895–896, 56–64. doi:10.1016/j.jchromb.2012.03.014
- 637 Özdemir, M., Crewe, K. H., Tucker, G. T., and Rostami-Hodjegan, A. (2004). Assessment of In Vivo
638 CYP2D6 Activity: Differential Sensitivity of Commonly Used Probes to Urine pH. *The Journal of*
639 *Clinical Pharmacology* 44, 1398–1404. doi:10.1177/0091270004269582
- 640 Pope, L. E., Khalil, M. H., Berg, J. E., Stiles, M., Yakatan, G. J., and Sellers, E. M. (2004).
641 Pharmacokinetics of Dextromethorphan After Single or Multiple Dosing in Combination With
642 Quinidine in Extensive and Poor Metabolizers. *The Journal of Clinical Pharmacology* 44, 1132–1142.
643 doi:10.1177/0091270004269521
- 644 Preskorn, S. H., Kane, C. P., Lobello, K., Nichols, A. I., Fayyad, R., Buckley, G., et al. (2013). Cytochrome
645 P450 2D6 phenoconversion is common in patients being treated for depression: Implications for
646 personalized medicine. *The Journal of clinical psychiatry* 74, 614–621. doi:10.4088/JCP.12m07807
- 647 Qiu, F., Liu, S., Miao, P., Zeng, J., Zhu, L., Zhao, T., et al. (2016). Effects of the Chinese herbal
648 formula "Zuojin Pill" on the pharmacokinetics of dextromethorphan in healthy Chinese volunteers with

- 649 CYP2D6*10 genotype. *European journal of clinical pharmacology* 72, 689–695. doi:10.1007/s00228-0
650 16-2048-7
- 651 Rau, T., Wohlleben, G., Wuttke, H., Thuerauf, N., Lunkenheimer, J., Lanczik, M., et al. (2004). CYP2D6
652 genotype: Impact on adverse effects and nonresponse during treatment with antidepressants-a pilot study.
653 *Clinical pharmacology and therapeutics* 75, 386–393. doi:10.1016/j.clpt.2003.12.015
- 654 [Dataset] RNAO (2022). Nursing best practice guideline by nurses' association of ontario: Appendix g:
655 Tools for assessing anxiety, depression, and stress. <https://bpgmobile.rnao.ca/sites/default/files/Appendix%20C%20Vein%20Anatomy.pdf>. Accessed: 2022-08-23
- 657 Rougée, L. R. A., Mohutsky, M. A., Bedwell, D. W., Ruterbories, K. J., and Hall, S. D. (2016). The
658 Impact of the Hepatocyte-to-Plasma pH Gradient on the Prediction of Hepatic Clearance and Drug-Drug
659 Interactions for CYP2D6 Substrates. *Drug metabolism and disposition: the biological fate of chemicals*
660 44, 1819–1827. doi:10.1124/dmd.116.071761
- 661 Rüdesheim, S., Selzer, D., Fuhr, U., Schwab, M., and Lehr, T. (2022). Physiologically-based
662 pharmacokinetic modeling of dextromethorphan to investigate interindividual variability within CYP2D6
663 activity score groups. *CPT: Pharmacometrics & Systems Pharmacology* n/a. doi:10.1002/psp4.12776
- 664 Sager, J. E., Lutz, J. D., Foti, R. S., Davis, C., Kunze, K. L., and Isoherranen, N. (2014). Fluoxetine-
665 and norfluoxetine-mediated complex drug-drug interactions: In vitro to in vivo correlation of effects on
666 CYP2D6, CYP2C19, and CYP3A4. *Clinical pharmacology and therapeutics* 95, 653–662. doi:10.1038/clpt.2014.50
- 668 Saravanakumar, A., Sadighi, A., Ryu, R., and Akhlaghi, F. (2019). Physicochemical Properties,
669 Biotransformation, and Transport Pathways of Established and Newly Approved Medications: A
670 Systematic Review of the Top 200 Most Prescribed Drugs vs. the FDA-Approved Drugs Between
671 2005 and 2016. *Clinical Pharmacokinetics* 58, 1281–1294. doi:10.1007/s40262-019-00750-8
- 672 Schadel, M., Wu, D., Otton, S. V., Kalow, W., and Sellers, E. M. (1995). Pharmacokinetics of
673 dextromethorphan and metabolites in humans: Influence of the CYP2D6 phenotype and quinidine
674 inhibition. *Journal of Clinical Psychopharmacology* 15, 263–269. doi:10.1097/00004714-199508000-0
675 0005
- 676 Schoedel, K. A., Pope, L. E., and Sellers, E. M. (2012). Randomized Open-Label Drug-Drug Interaction
677 Trial of Dextromethorphan/Quinidine and Paroxetine in Healthy Volunteers:. *Clinical Drug Investigation*
678 32, 157–169. doi:10.2165/11599870-00000000-00000
- 679 Shah, R. R. and Smith, R. L. (2015). Addressing phenoconversion: The Achilles' heel of personalized
680 medicine: Impact of phenoconversion. *British Journal of Clinical Pharmacology* 79, 222–240. doi:10.1
681 111/bcp.12441
- 682 Silva, A. R. and Dinis-Oliveira, R. J. (2020). Pharmacokinetics and pharmacodynamics of
683 dextromethorphan: Clinical and forensic aspects. *Drug Metabolism Reviews* 52, 258–282. doi:10
684 .1080/03602532.2020.1758712
- 685 Somogyi, E. T., Bouteiller, J.-M., Glazier, J. A., König, M., Medley, J. K., Swat, M. H., et al. (2015).
686 libRoadRunner: A high performance SBML simulation and analysis library. *Bioinformatics (Oxford, England)* 31, 3315–3321. doi:10.1093/bioinformatics/btv363
- 688 Steinberg, G. K., Bell, T. E., and Yenari, M. A. (1996). Dose escalation safety and tolerance study of the
689 N-methyl-d-aspartate antagonist dextromethorphan in neurosurgery patients. *Journal of Neurosurgery*
690 84, 860–866. doi:10.3171/jns.1996.84.5.0860
- 691 Storelli, F., Desmeules, J., and Daali, Y. (2019a). Genotype-sensitive reversible and time-dependent
692 CYP2D6 inhibition in human liver microsomes. *Basic & clinical pharmacology & toxicology* 124,
693 170–180. doi:10.1111/bcpt.13124

- 694 Storelli, F., Desmeules, J., and Daali, Y. (2019b). Physiologically-Based Pharmacokinetic Modeling for
695 the Prediction of CYP2D6-Mediated Gene–Drug–Drug Interactions. *CPT: Pharmacometrics & Systems*
696 *Pharmacology* 8, 567–576. doi:10.1002/psp4.12411
- 697 Strauch, K., Lutz, U., Bittner, N., and Lutz, W. K. (2009). Dose–response relationship for the
698 pharmacokinetic interaction of grapefruit juice with dextromethorphan investigated by human urinary
699 metabolite profiles. *Food and Chemical Toxicology* 47, 1928–1935. doi:10.1016/j.fct.2009.05.004
- 700 Takashima, T., Murase, S., Iwasaki, K., and Shimada, K. (2005). Evaluation of Dextromethorphan
701 Metabolism Using Hepatocytes from CYP2D6 Poor and Extensive Metabolizers. *Drug Metabolism and*
702 *Pharmacokinetics* 20, 177–182. doi:10.2133/dmpk.20.177
- 703 Tamminga, W., Wemer, J., Oosterhuis, B., de Zeeuw, R., de Leij, L., and Jonkman, J. (2001). The
704 prevalence of CYP2D6 and CYP2C19 genotypes in a population of healthy Dutch volunteers. *European*
705 *Journal of Clinical Pharmacology* 57, 717–722. doi:10.1007/s002280100359
- 706 Taylor, C. P., Traynelis, S. F., Siffert, J., Pope, L. E., and Matsumoto, R. R. (2016). Pharmacology of
707 dextromethorphan: Relevance to dextromethorphan/quinidine (Nuedexta®) clinical use. *Pharmacology*
708 & *Therapeutics* 164, 170–182. doi:10.1016/j.pharmthera.2016.04.010
- 709 Tennezé, L., Verstuyft, C., Becquemont, L., Poirier, J. M., Wilkinson, G. R., and Funck-Brentano,
710 C. (1999). Assessment of CYP2D6 and CYP2C19 activity in vivo in humans: A cocktail study
711 with dextromethorphan and chloroguanide alone and in combination. *Clinical Pharmacology and*
712 *Therapeutics* 66, 582–588. doi:10.1053/cp.1999.v66.103401001
- 713 Tricco, A. C., Lillie, E., Zarin, W., O'Brien, K. K., Colquhoun, H., Levac, D., et al. (2018). PRISMA
714 Extension for Scoping Reviews (PRISMA-ScR): Checklist and Explanation. *Annals of Internal Medicine*
715 169, 467–473. doi:10.1053/gfd.8vk
- 716 Vander, J. S., A. (2001). Human physiology: The mechanisms of body function. *McGraw-Hill higher*
717 *education*
- 718 von Moltke, L. L., Greenblatt, D. J., Grassi, J. M., Granda, B. W., Venkatakrishnan, K., Schmider, J., et al.
719 (1998). Multiple human cytochromes contribute to biotransformation of dextromethorphan in-vitro:
720 Role of CYP2C9, CYP2C19, CYP2D6, and CYP3A. *The Journal of Pharmacy and Pharmacology* 50,
721 997–1004. doi:10.1111/j.2042-7158.1998.tb06914.x
- 722 Whirl-Carrillo, M., Huddart, R., Gong, L., Sangkuhl, K., Thorn, C. F., Whaley, R., et al. (2021). An
723 evidence-based framework for evaluating pharmacogenomics knowledge for personalized medicine.
724 *Clinical pharmacology and therapeutics* 110, 563–572. doi:10.1002/cpt.2350
- 725 Wyen, C., Fuhr, U., Frank, D., Aarnoutse, R. E., Klaassen, T., Lazar, A., et al. (2008). Effect of an
726 antiretroviral regimen containing ritonavir boosted lopinavir on intestinal and hepatic CYP3A, CYP2D6
727 and P-glycoprotein in HIV-infected patients. *Clinical pharmacology and therapeutics* 84, 75–82.
728 doi:10.1038/sj.clpt.6100452
- 729 Yamazaki, T., Desai, A., Goldwater, R., Han, D., Howieson, C., Akhtar, S., et al. (2017). Pharmacokinetic
730 Effects of Isavuconazole Coadministration With the Cytochrome P450 Enzyme Substrates Bupropion,
731 Repaglinide, Caffeine, Dextromethorphan, and Methadone in Healthy Subjects. *Clinical pharmacology*
732 *in drug development* 6, 54–65. doi:10.1002/cpdd.281
- 733 Yang, J., He, M. M., Niu, W., Wrighton, S. A., Li, L., Liu, Y., et al. (2012). Metabolic capabilities
734 of cytochrome P450 enzymes in Chinese liver microsomes compared with those in Caucasian liver
735 microsomes: Hepatic cytochromes P450 of Chinese and Caucasians. *British Journal of Clinical*
736 *Pharmacology* 73, 268–284. doi:10.1111/j.1365-2125.2011.04076.x

- 737 Yu, A. and Haining, R. L. (2001). Comparative contribution to dextromethorphan metabolism by
738 cytochrome P450 isoforms in vitro: Can dextromethorphan be used as a dual probe for both CYP2D6 and
739 CYP3A activities? *Drug Metabolism and Disposition: The Biological Fate of Chemicals* 29, 1514–1520
- 740 Zackrisson, A. L., Lindblom, B., and Ahlner, J. (2010). High Frequency of Occurrence of CYP2D6
741 Gene Duplication/Multiduplication Indicating Ultrarapid Metabolism Among Suicide Cases. *Clinical*
742 *Pharmacology & Therapeutics* 88, 354–359. doi:10.1038/clpt.2009.216
- 743 Zanger, U. M., Raimundo, S., and Eichelbaum, M. (2004). Cytochrome P450 2D6: Overview and update on
744 pharmacology, genetics, biochemistry. *Naunyn-Schmiedeberg's archives of pharmacology* 369, 23–37.
745 doi:10.1007/s00210-003-0832-2
- 746 Zawertailo, L. A., Tyndale, R. F., Bustos, U., and Sellers, E. M. (2010). Effect of metabolic blockade on the
747 psychoactive effects of dextromethorphan. *Human Psychopharmacology: Clinical and Experimental* 25,
748 71–79. doi:10.1002/hup.1086

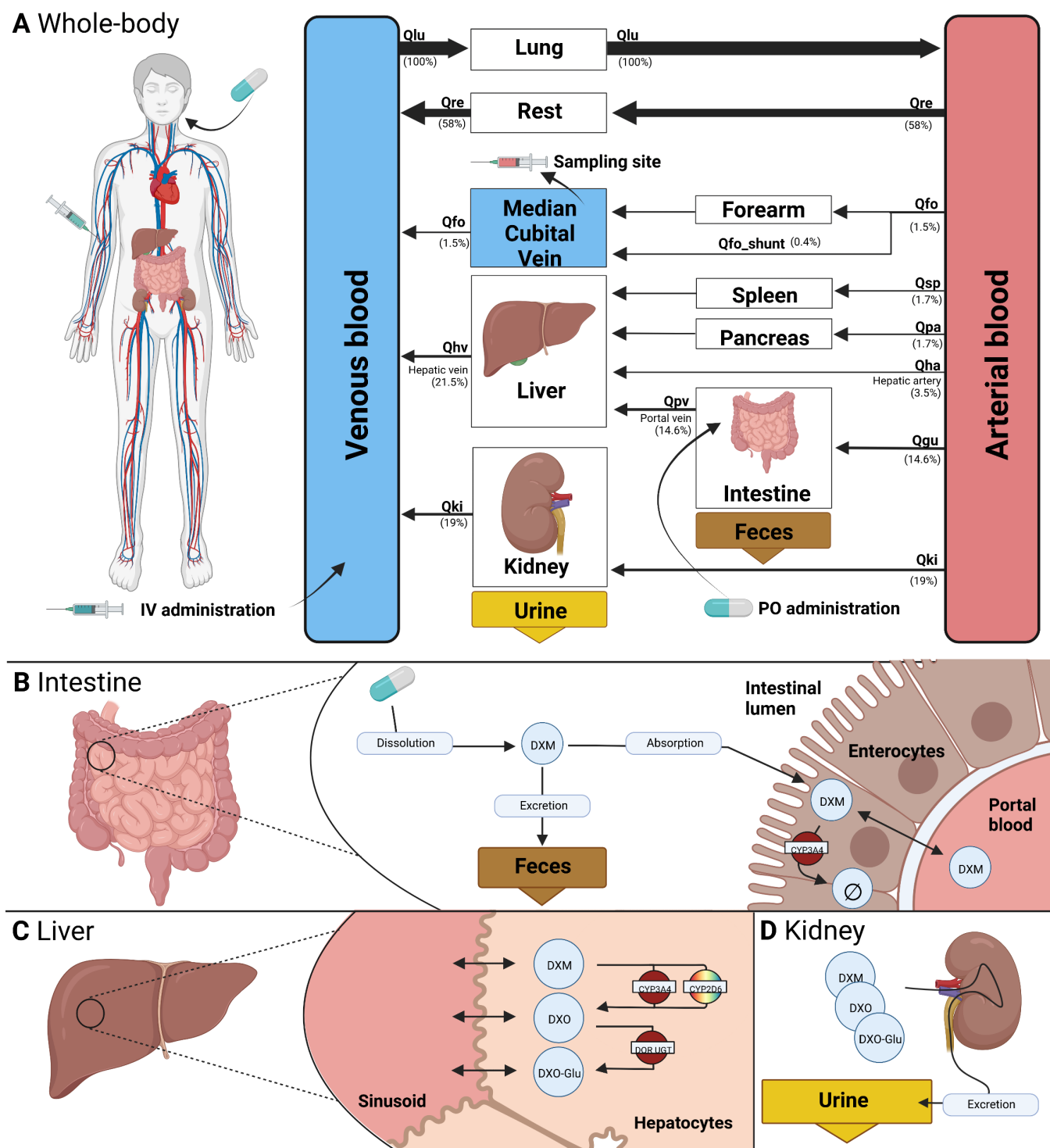


Figure 1. PBPK model of dextromethorphan (DXM). **A**) whole body model consisting of liver, kidney, intestine, forearm, lung and the rest compartment. Organs with minor relevance are not modeled explicitly and lumped into the rest compartment. Organs are coupled via the systemic circulation with arrow width proportional to relative blood flow. DXM can be administered intravenously (IV) or orally (PO) with DXM appearing in the venous blood or intestine, respectively. **B**) intestine model consisting of dissolution, absorption and excretion of DXM. Only a fraction of DXM is absorbed with the remainder excreted in the feces. First pass metabolism of DXM via CYP3A4 in the intestine reduces the amount of DXM appearing in the circulation. **C**) liver model consisting of $\text{DXM} \rightarrow \text{DXO}$ conversion via CYP2D6 and CYP3A4 and subsequent glucuronidation to DXO-Glu. **D**) kidney model for the urinary excretion of DXM, DXO and DXO-Glu. Created with BioRender.com.

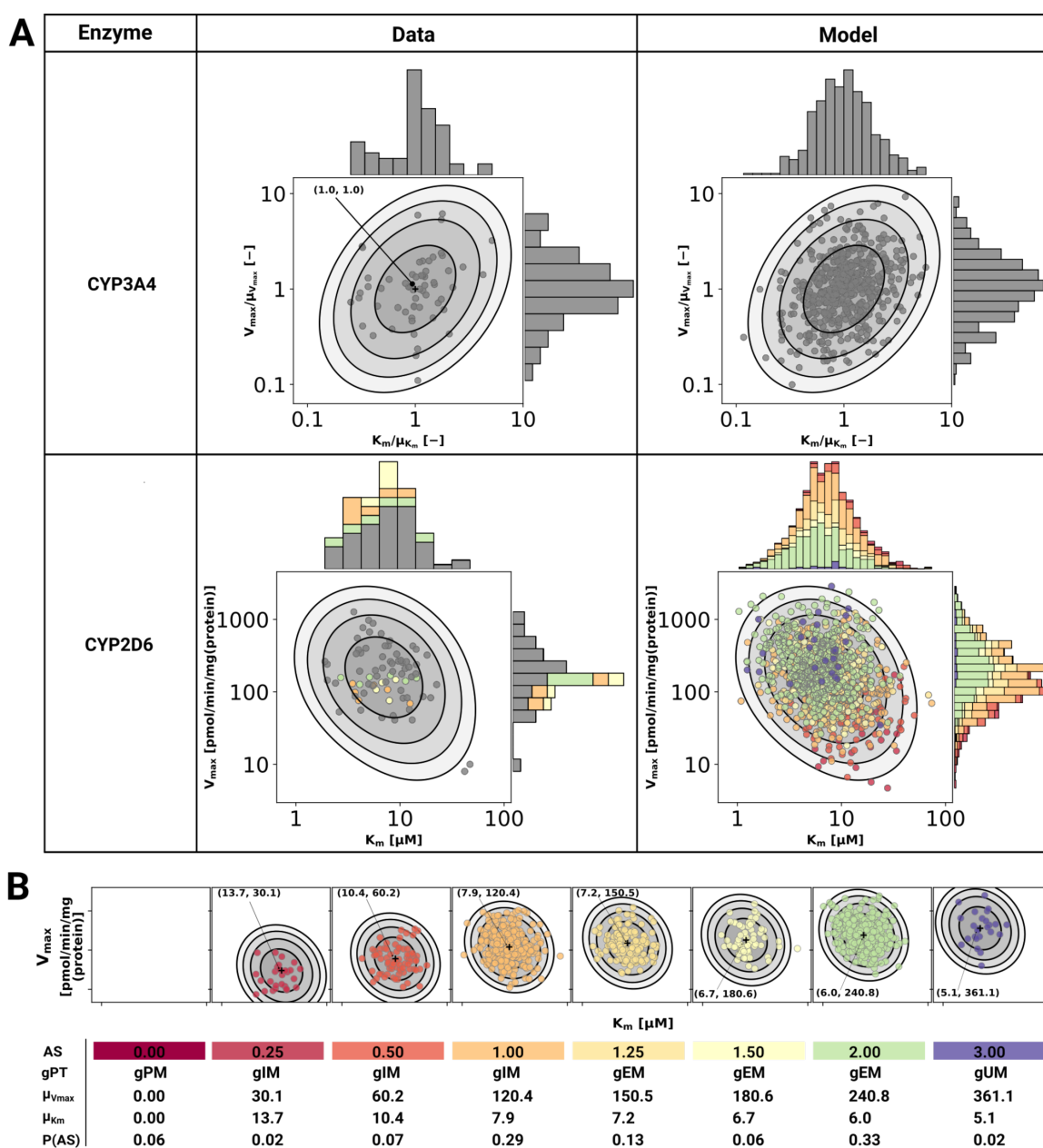


Figure 2. Model of CYP3A4 and CYP2D6. A) CYP3A4 and CYP2D6 distributions. Conversion of DXM → DXO via CYP3A4 and CYP2D6 are modeled via Michaelis-Menten kinetics. Variability was included via two-dimensional lognormal distributions of Michaelis-Menten coefficient (K_m) and maximum rate of reaction (V_{max}). The distribution parameters were determined by fitting to in vitro data in human liver microsomes. Variability of CYP3A4 parameters was measured by midazolam (Yang et al., 2012), variability of CYP2D6 parameters via DXM (Yang et al., 2012; Storelli et al., 2019a). To transfer the CYP3A4 data from midazolam to DXM normalized values were used. The distribution of CYP2D6 was modeled as a mixture model of the underlying activity scores as depicted in B. The model CYP3A4 and CYP2D6 distributions were sampled with each point corresponding to a combination of V_{max} and K_m . CYP2D6 data was color-coded by the respective activity score. B) CYP2D6 activity score model. CYP2D6 activity was modeled via a mixture model of individual activity scores. With increasing activity score the V_{max} for the DXM → DXO conversion increases and the μ_{Km} for DXM decreases, i.e., reaction velocity and affinity for the substrate increase. The table provides AS, genetic phenotype (gPT), mean V_{max} , mean K_m , and AS frequency in curated UCMR data (P(AS)). In case of AS=0.0 CYP2D6 has no activity for the DXM → DXO conversion.

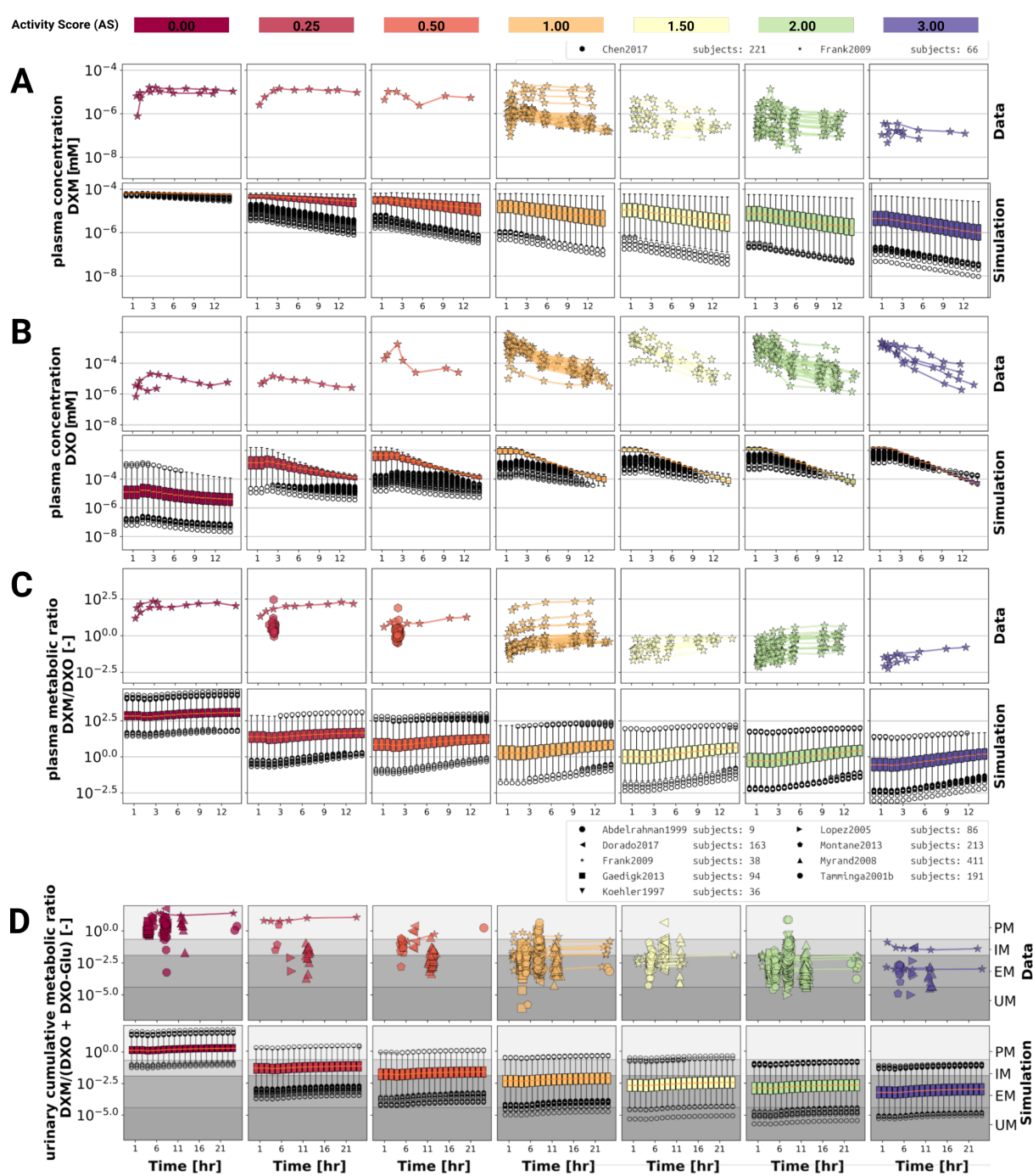


Figure 3. Time-dependency of DXM pharmacokinetics by activity score. A) DXM plasma concentration, B) DXO plasma concentration, C) DXM/DXO plasma ratio, D) UCMR (DXM/(DXM+DXO+Glu) in urine) Depicted is the subset of data in which 30 mg of DXM was applied orally. The upper rows in the panels depict the data in healthy adults from (Abdelrahman et al., 1999; Chen et al., 2017; Dorado et al., 2017; Frank, 2009; Gaedigk, 2013; Köhler et al., 1997; López et al., 2005; Montané Jaime et al., 2013; Myrand et al., 2008; Tamminga et al., 2001). Cocktail studies are included. Studies containing coadministrations with established drug-drug interactions are excluded. The lower rows depict the respective simulation results. To visualize the large variability in the simulation box plots showing the quartiles along side the median and outliers for selected time points are used. Variables changed in the simulation are the CYP3A4 and CYP2D6 reaction parameters K_m and V_{max} according to the distributions in Fig. 2. For the different activity scores the respective CYP2D6 activity score model was used.

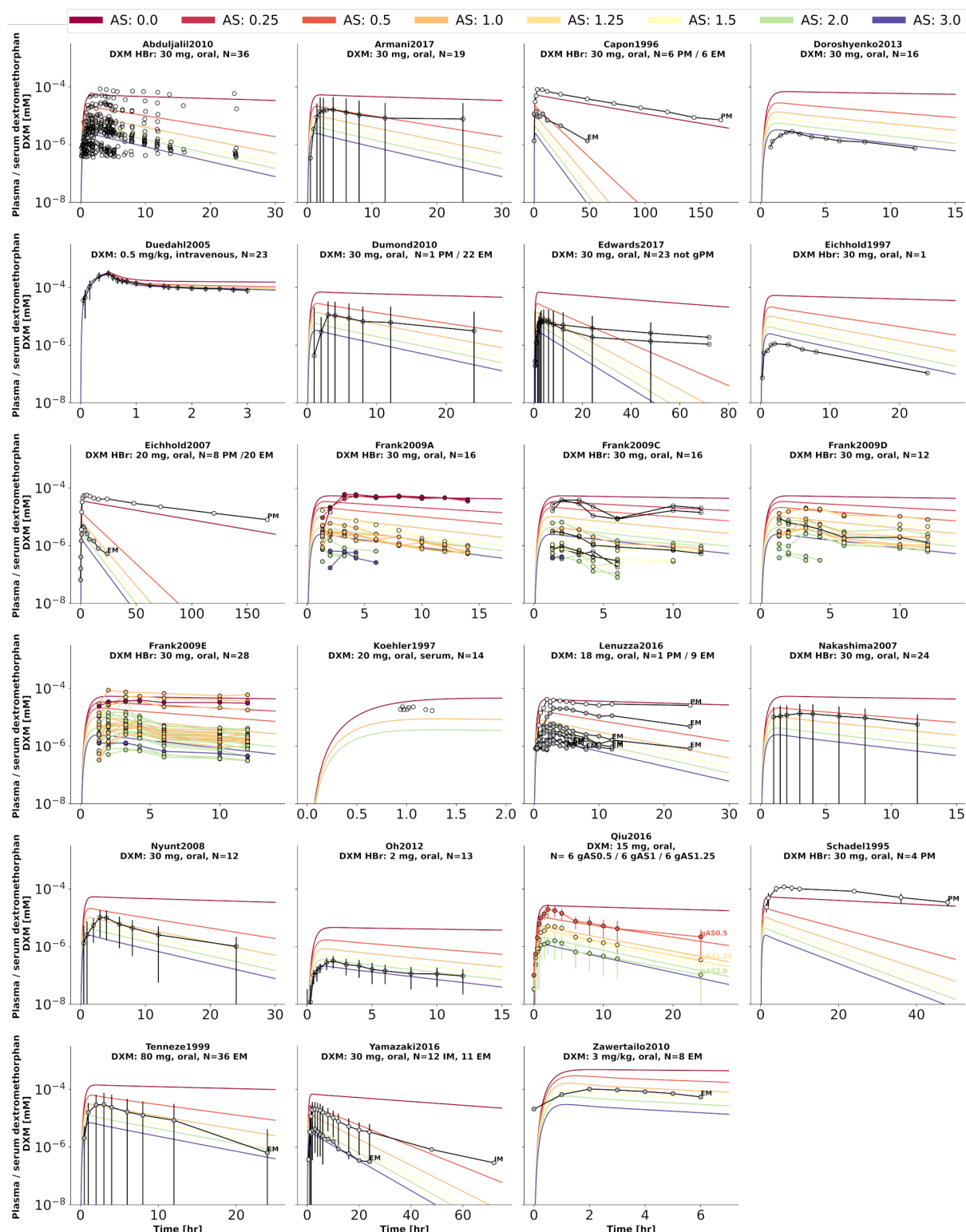


Figure 4. Dextromethorphan (DXM) concentration in plasma or serum. Studies were simulated according to the reported dosing protocol. In case of available activity score information the clinical data is color coded accordingly. Information on metabolizer phenotype (UM, EM, IM, PM) is provided where reported. Data from (Abduljalil et al., 2010; Armani et al., 2017; Capon et al., 1996; Doroshyenko et al., 2013; Duedahl et al., 2005; Dumond et al., 2010; Edwards et al., 2017; Eichhold et al., 1997, 2007; Frank, 2009; Köhler et al., 1997; Lenuzza et al., 2016; Nakashima et al., 2007; Nyunt et al., 2008; Oh et al., 2012; Qiu et al., 2016; Schadel et al., 1995; Tennezé et al., 1999; Yamazaki et al., 2017; Zawertailo et al., 2010).

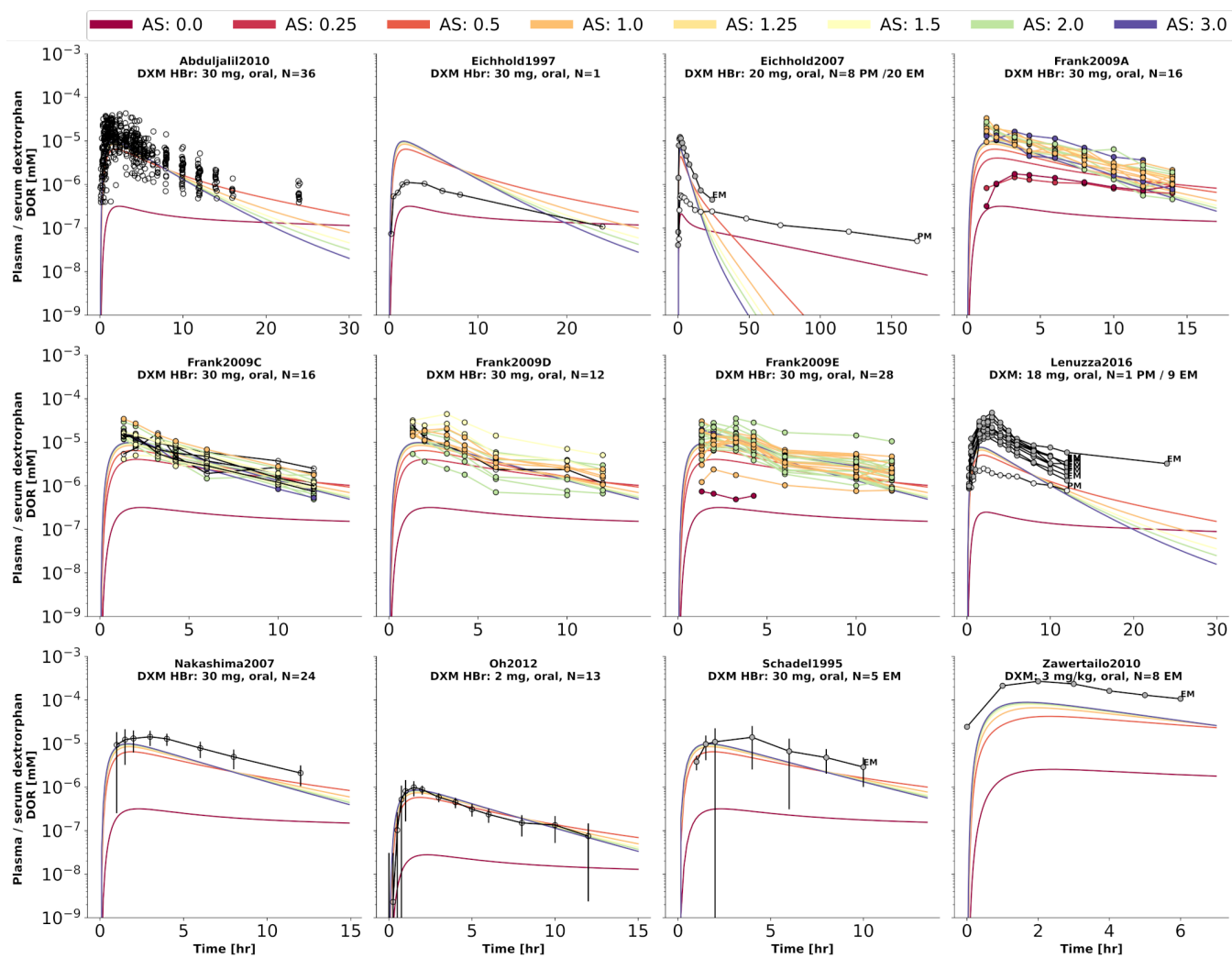


Figure 5. Dextrophen (DXO) concentration in plasma or serum. Studies were simulated according to the reported dosing protocol. In case of available activity score information the clinical data is color coded accordingly. Information on metabolizer phenotype (UM, EM, IM, PM) is provided where reported. Data from (Abduljalil et al., 2010; Eichhold et al., 1997, 2007; Frank, 2009; Lenuzza et al., 2016; Nakashima et al., 2007; Oh et al., 2012; Schadel et al., 1995; Zawertailo et al., 2010).

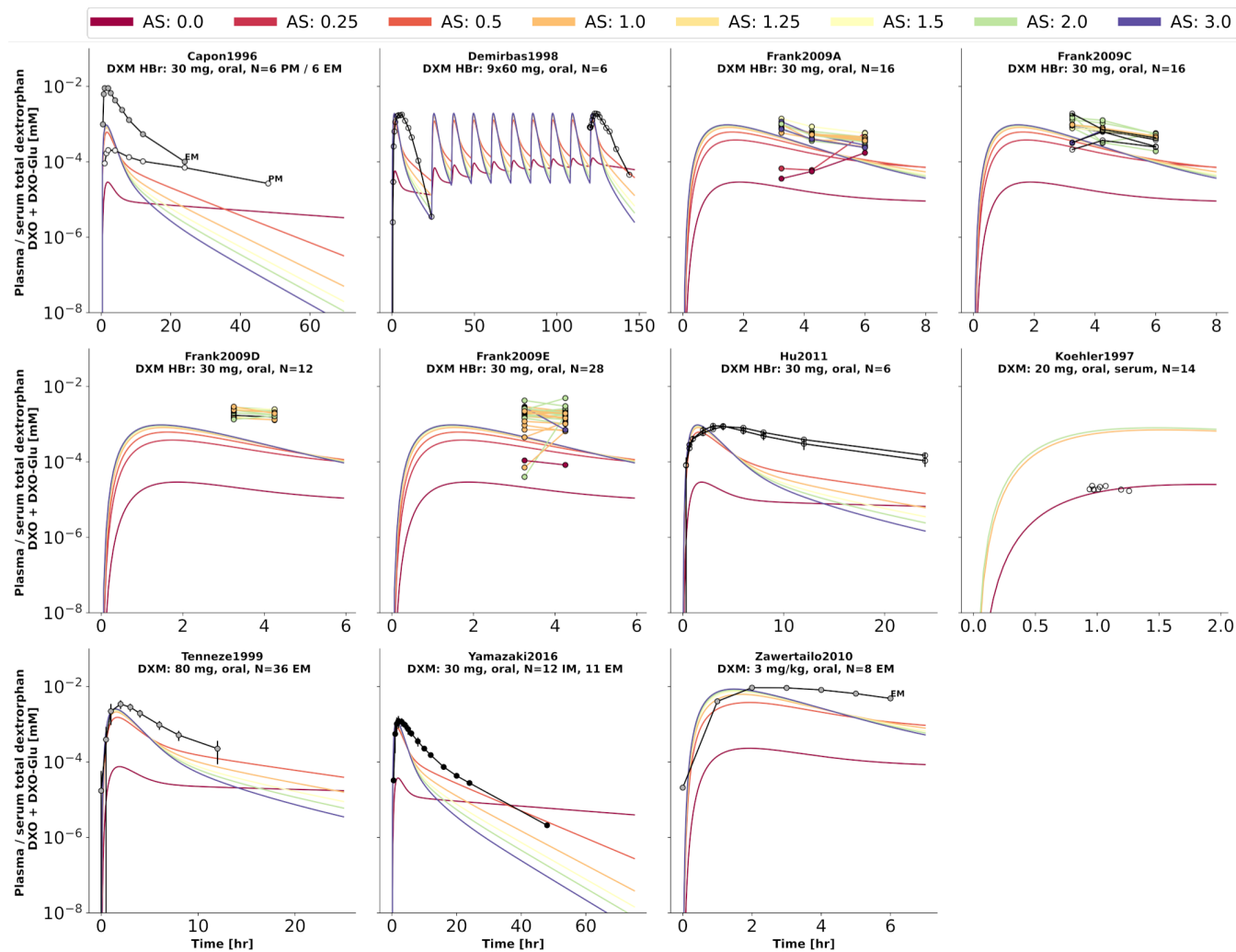


Figure 6. Total dextrorphan (DXO+DXO-Glu) concentration in plasma or serum. Studies were simulated according to the reported dosing protocol. In case of available activity score information the clinical data is color coded accordingly. Information on metabolizer phenotype (UM, EM, IM, PM) is provided where reported. Data from (Capon et al., 1996; Demirbas et al., 1998; Hu et al., 2011; Köhler et al., 1997; Tenneze et al., 1999; Yamazaki et al., 2017; Zawertailo et al., 2010).

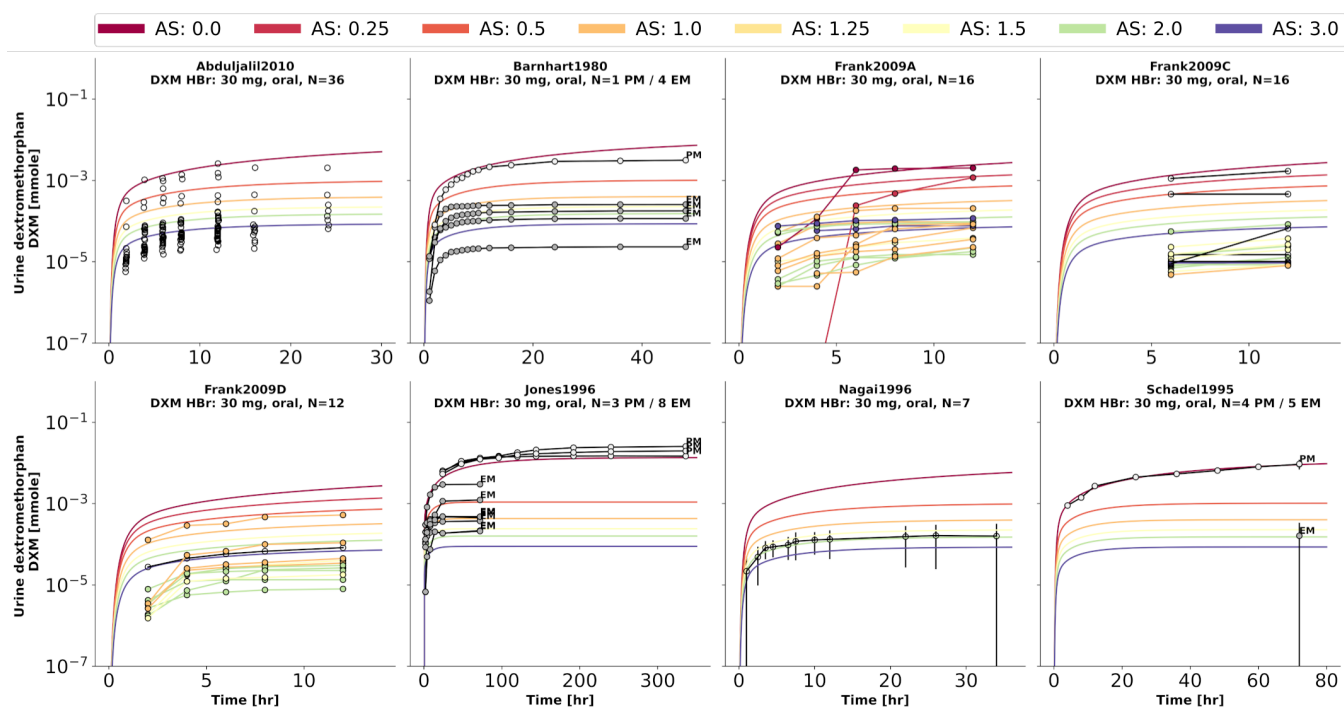


Figure 7. Dextromethorphan (DXM) amount in urine. Studies were simulated according to the reported dosing protocol. In case of available activity score information the clinical data is color coded accordingly. Information on metabolizer phenotype (UM, EM, IM, PM) is provided where reported. Data from (Abduljalil et al., 2010; Barnhart, 1980; Frank, 2009; Jones et al., 1996; Nagai et al., 1996; Schadel et al., 1995).

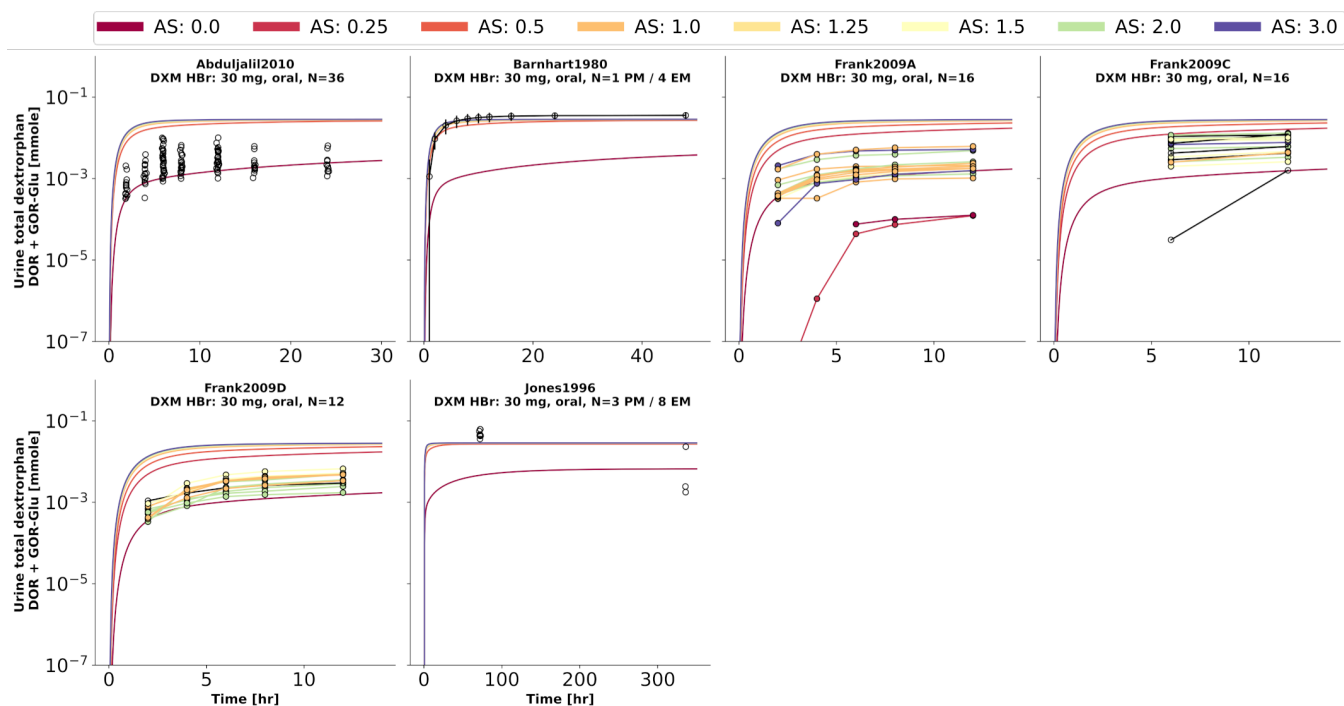


Figure 8. Total dextrophan (DXO+DXO-Glu) amount in urine. Studies were simulated according to the reported dosing protocol. In case of available activity score information the clinical data is color coded accordingly. Information on metabolizer phenotype (UM, EM, IM, PM) is provided where reported. Data from (Abduljalil et al., 2010; Barnhart, 1980; Frank, 2009; Jones et al., 1996).

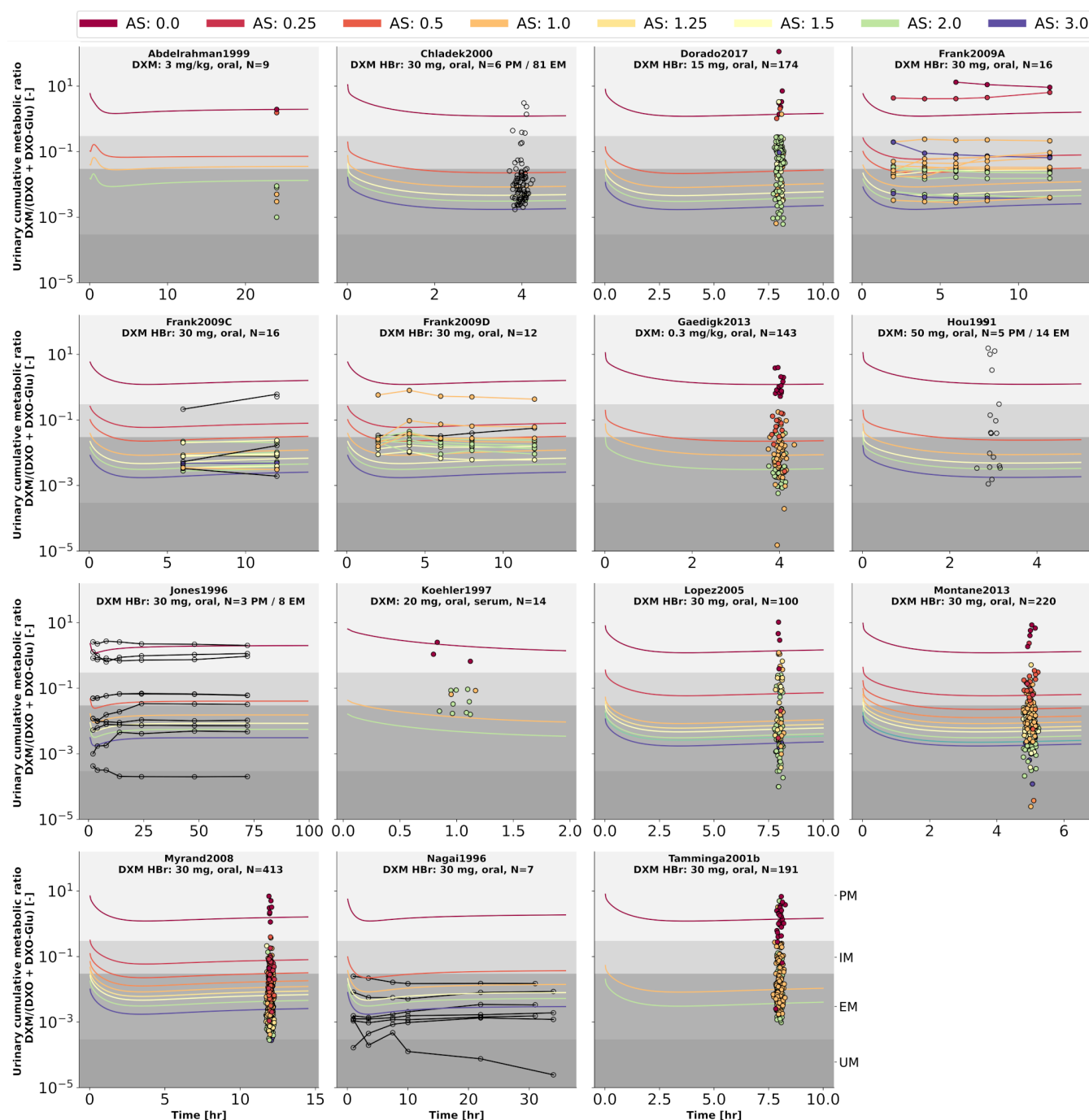


Figure 9. Cumulative metabolic ratio between dextromethorphan and total dextrorphan ($\text{DXM}/(\text{DXO} + \text{DXO-GLU})$) in urine (UCMR). Studies were simulated according to the reported dosing protocol. In case of available activity score information the clinical data is color coded accordingly. Information on metabolizer phenotype (UM, EM, IM, PM) is provided where reported. Data from (Abdelrahman et al., 1999; Chládek et al., 2000; Dorado et al., 2017; Frank, 2009; Gaedigk, 2013; Hou et al., 1991; Jones et al., 1996; Köhler et al., 1997; López et al., 2005; Montané Jaime et al., 2013; Myrand et al., 2008; Nagai et al., 1996; Tamminga et al., 2001). The metabolic phenotype definitions for UM, EM, IM, PM are depicted as gray areas.

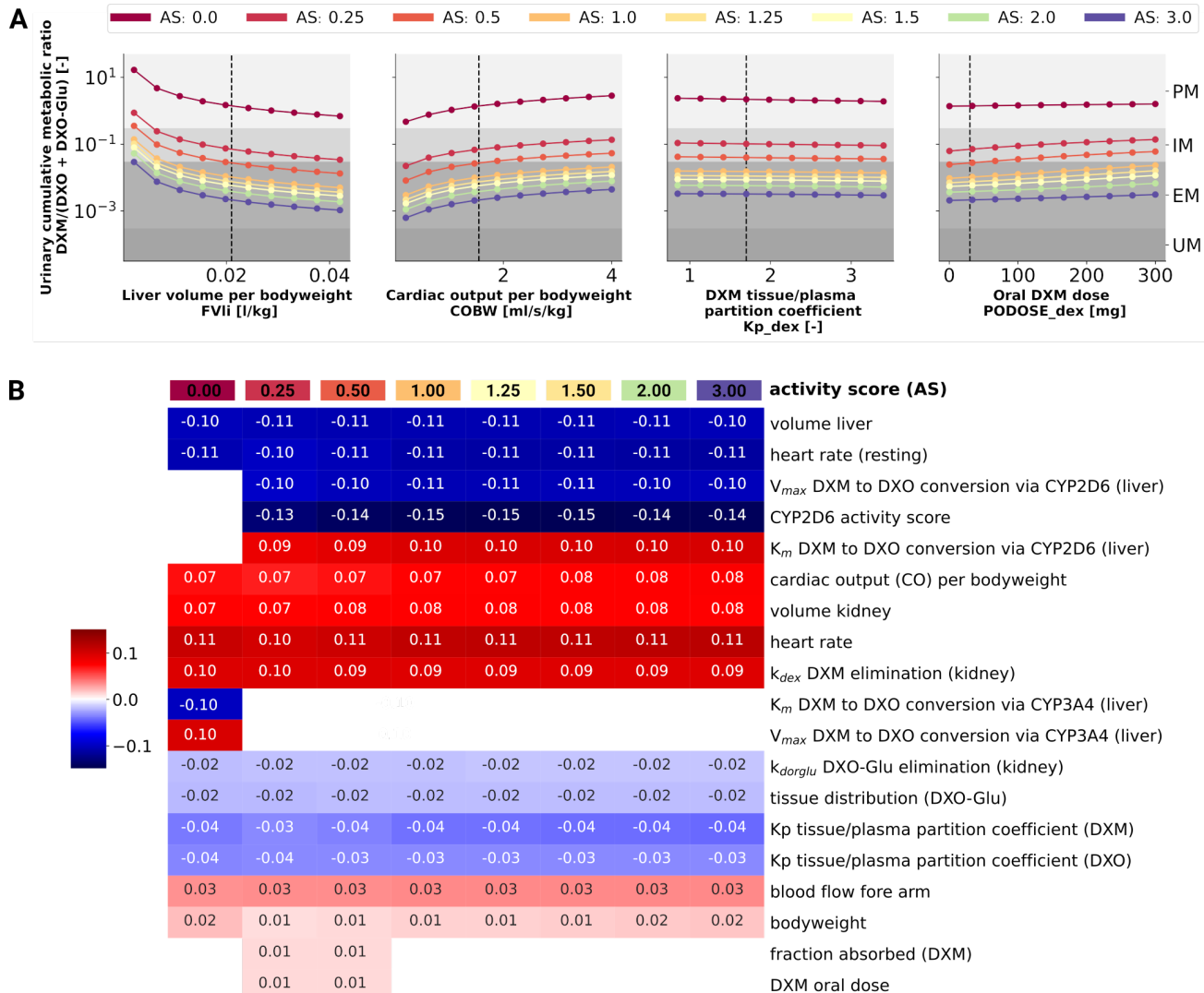


Figure 10. Sensitivity analysis of UCMR by activity score. **A)** Dependency of UCMR (urinary cumulative ratio of DXM/(DXO-Glu)) after 8 hr and 30 mg oral DXM) on selected physiological parameters and the DXM dose. Parameter scans were performed for all activity scores. Reference model parameters are depicted as dashed lines. **B)** Sensitivity analysis of model parameters. To systematically study the effect of parameter changes the local sensitivity of UCMR were calculated for all activity scores. Parameters were varied 10% in both direction around the reference parameter value and the relative change of UCMR was calculated (insensitive parameters with relative change of UCMR smaller than 1% were omitted). Positive sensitivities are depicted in red, negative sensitivities in blue. Parameters were sorted via agglomerative clustering. Representative parameters of the clusters (i.e. liver volume per bodyweight, cardiac output per bodyweight, DXM tissue/plasma partition coefficient, and oral DXM dose) are depicted in A. The local sensitivity for the activity scores in B corresponds to the normalized slope at the dashed lines in A.

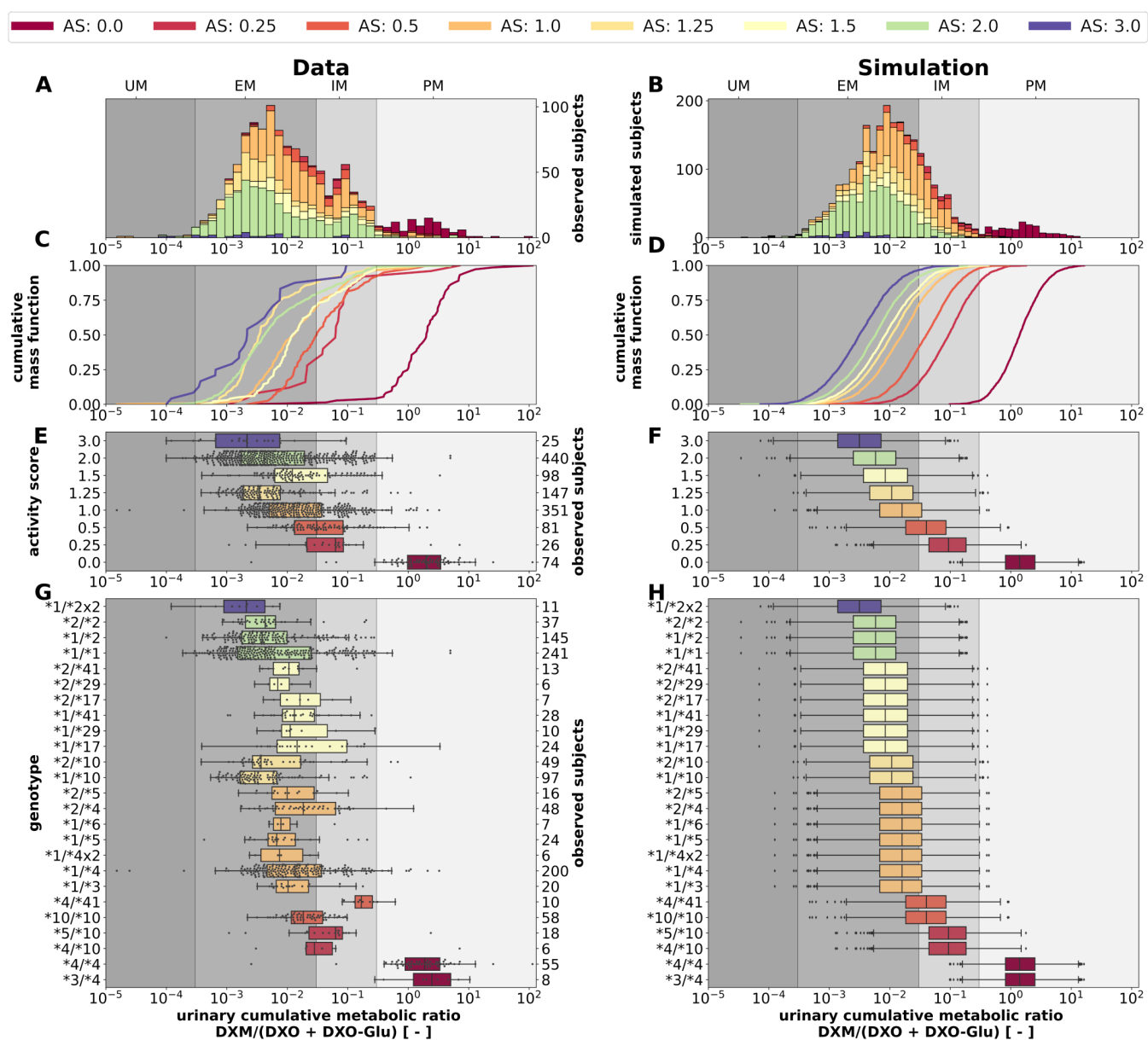


Figure 11. CYP2D6 genotype-, activity score association of the UCMR. Simulation of urinary cumulative ratio of DXM/(DXO-Glu) (UCMR) based on activity score frequencies. UCMR data was measured at least 4hr after the application of DXM (hydrobromide) in healthy adults. Cocktail studies were included in the analysis. Studies containing coadministrations with established drug-drug interactions were excluded. The ranges for metabolic phenotypes (UM, EM, IM, PM) are depicted as gray shaded areas. For timecourse UCMRs, only the latest measurement after administration was included. Data from (Abdelrahman et al., 1999; Dorado et al., 2017; Frank, 2009; Gaedigk, 2013; Köhler et al., 1997; López et al., 2005; Montané Jaime et al., 2013; Myrand et al., 2008; Tamminga et al., 2001). **A)** Histogram of UCMR data stratified by CYP2D6 activity score. **B)** Corresponding simulation results (UCMR at 8hr) from the Monte Carlo simulation with random variables being the enzyme reaction parameter (i.e. K_m , V_{max}). See details in Fig. 2. **C)** Empirical CMFs stratified by the activity scores. **D)** Corresponding simulated CMFs stratified by CYP2D6 activity scores. **E)** Box plots of observed UCMRs stratified by CYP2D6 activity scores. **F)** Box plots of simulated UCMRs stratified by the activity scores. **G)** Box plots of observed UCMRs stratified by CYP2D6 diplotypes. **H)** Box plots of simulated UCMRs stratified by CYP2D6 diplotypes. For D, F, and H, 2000 samples were simulated for each activity score whereas in B and D a two-fold oversampling with the CYP2D6 activity score frequencies from the UCMR data was performed.

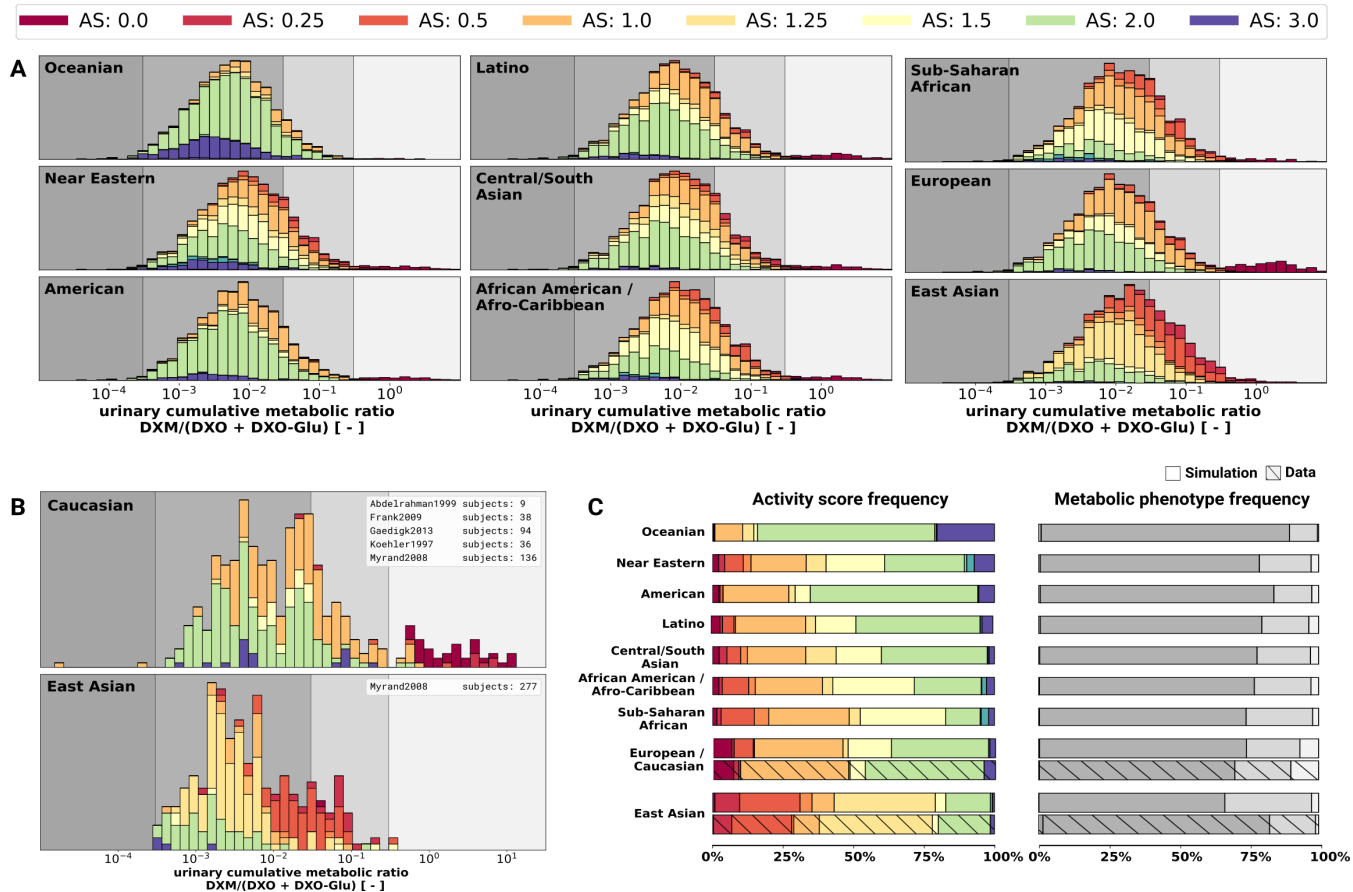


Figure 12. UCMR distributions for biogeographical populations **A)** Simulated UCMR distributions at 8hr for various biogeographical populations based on reported CYP2D6 activity score frequencies as reported in PharmGKB (Whirl-Carrillo et al., 2021). Frequencies are provided in the Supplementary Tab. S2. **B)** Reported UCMRs depending on activity score for Caucasians and East Asians from (Abdelrahman et al., 1999; Frank, 2009; Gaedigk, 2013; Köhler et al., 1997; Myrand et al., 2008). Cocktail studies were included in the analysis. Studies containing coadministrations with established drug-drug interactions were excluded. **C)** Simulated activity score frequency and metabolic phenotype frequency for the populations and comparison with data for Caucasian and East Asian populations (hatched bars).

Table 1 Clinical studies with pharmacokinetics used for model evaluation. NR: not reported, DXM: dextromethorphan.

| Reference | PK-DB | PMID | DXM application | Dosing protocol | Description |
|----------------------------|-----------|----------|--------------------------------|--|---|
| Abdelrahman et al. (1999) | PKDB00573 | 10340911 | DXM | Oral (syrup): 0.3 mg/kg | Investigation of terbinafine as a CYP2D6 inhibitor in vivo. |
| Abduljalil et al. (2010) | PKDB00574 | 20881950 | DXM hydrobromide | Oral (capsule): 30 mg | Assessment of activity levels for CYP2D6*1, CYP2D6*2, and CYP2D6*41 genes by population pharmacokinetics of dextromethorphan. |
| Armani et al. (2017) | PKDB00428 | 10340911 | DXM (in cocktail) | Oral (NR): 30 mg | The antitussive effect of dextromethorphan in relation to CYP2D6 activity. |
| Barnhart (1980) | PKDB00575 | 7423506 | DXM hydrobromide | Oral (capsule): 30 mg | The urinary excretion of dextromethorphan and three metabolites in dogs and humans. |
| Capon et al. (1996) | PKDB00576 | 8841152 | DXM hydrobromide | Oral (NR): 30 mg | The antitussive effect of dextromethorphan in relation to CYP2D6 activity. |
| Chen et al. (2017) | PKDB00577 | 28512430 | DXM | Oral (tablet): 15 mg + water 300ml | CYP2D6 phenotyping using urine, plasma, and saliva metabolic ratios to assess the impact of CYP2D6*10 on inter-individual variation in a Chinese population. |
| Chládek et al. (2000) | PKDB00578 | 11214771 | DXM hydrobromide | Oral (syrup): 30 mg | In-vivo indices of CYP2D6 activity: comparison of dextromethorphan metabolic ratios in 4-h urine and 3-h plasma. |
| Demirbas et al. (1998) | PKDB00579 | 9840216 | DXM hydrobromide | Oral (sustained release tablet): 60 mg | Bioavailability of dextromethorphan (as dextrorphan) from sustained release formulations in the presence of guaifenesin in human volunteers. |
| Dorado et al. (2017) | PKDB00580 | 28271978 | DXM | Oral (NR): 15 mg | Lessons from Cuba for global precision medicine: CYP2D6 genotype is not a robust predictor of CYP2D6 ultrarapid metabolism. |
| Doroshchenko et al. (2013) | PKDB00138 | 23401474 | DXM (in cocktail) | Oral (capsule): 30 mg | Drug metabolism and disposition: the biological fate of chemicals. |
| Duedahl et al. (2005) | PKDB00597 | 15661445 | DXM | Intravenous: 0.5 mg/kg | Intravenous dextromethorphan to human volunteers: relationship between pharmacokinetics and anti-hyperalgesic effect. |
| Dumond et al. (2010) | PKDB00499 | 20147896 | DXM (in cocktail) | Oral (solution): 30 mg | A phenotype-genotype approach to predicting CYP450 and P-glycoprotein drug interactions with the mixed inhibitor/inducer tipranavir/ritonavir. |
| Edwards et al. (2017) | PKDB00496 | 28808886 | DXM (in cocktail) | Oral (capsule): 30 mg | Assessment of pharmacokinetic interactions between obeticholic acid and caffeine, midazolam, warfarin, dextromethorphan, omeprazole, rosuvastatin, and digoxin in phase 1 studies in healthy subjects. |
| Eichhold et al. (1997) | PKDB00596 | - | DXM hydrobromide | Oral (syrup): 30 mg | Determination of dextromethorphan and dextrorphan in human plasma by liquid chromatography/tandem mass spectrometry. |
| Eichhold et al. (2007) | PKDB00581 | 16930908 | DXM hydrobromide | Oral (solution): 20 mg | Simultaneous determination of dextromethorphan, dextrorphan, and guaifenesin in human plasma using semi-automated liquid/liquid extraction and gradient liquid chromatography tandem mass spectrometry. |
| Frank (2009) | PKDB00582 | - | DXM hydrobromide (in cocktail) | Oral (capsule): 30 mg | Evaluation of pharmacokinetic metrics for phenotyping of the human CYP2D6 enzyme with dextromethorphan. |
| Gaedigk (2013) | PKDB00583 | 24151800 | DXM | Oral (syrup): 0.3 mg/kg | Complexities of CYP2D6 gene analysis and interpretation. |
| Hou et al. (1991) | PKDB00584 | 2015730 | DXM hydrobromide | Oral (capsule): 50 mg | Salivary analysis for determination of dextromethorphan metabolic phenotype. |
| Hu et al. (2011) | PKDB00585 | 21050887 | DXM hydrobromide | Oral (sustained release tablet): 30 mg | Floating matrix dosage form for dextromethorphan hydrobromide based on gas forming technique: in vitro and in vivo evaluation in healthy volunteers. |
| Jones et al. (1996) | PKDB00586 | 8873685 | DXM hydrobromide | Oral (syrup): 30 mg | Determination of cytochrome P450 3A4/5 activity in vivo with dextromethorphan N-demethylation. |
| Köhler et al. (1997) | PKDB00587 | 9429230 | DXM | Oral (syrup): 20 mg | CYP2D6 genotype and phenotyping by determination of dextromethorphan and metabolites in serum of healthy controls and of patients under psychotropic medication. |
| López et al. (2005) | PKDB00588 | 16249913 | DXM hydrobromide | Oral (syrup): 30 mg | CYP2D6 genotype and phenotype determination in a Mexican Mestizo population. |

(continued)

| Reference | PK-DB | PMID | DXM application | Dosing protocol | Description |
|-----------------------------|-----------|----------|-------------------|---|--|
| Lenuzza et al. (2016) | PKDB00598 | 25465228 | DXM (in cocktail) | Oral (tablet): 18 mg | Safety and pharmacokinetics of the (CIME) Combination of Drugs and Their Metabolites after a single oral dosing in healthy volunteers. |
| Montané Jaime et al. (2013) | PKDB00589 | 23394389 | DXM hydrobromide | Oral (NR): 30 mg + water | Characterization of the CYP2D6 gene locus and metabolic activity in Indo- and Afro-Trinidadians: discovery of novel allelic variants. |
| Myrand et al. (2008) | PKDB00497 | 18231117 | DXM (in cocktail) | Oral (NR): 30 mg | Pharmacokinetics/genotype associations for major cytochrome P450 enzymes in native and first- and third-generation Japanese populations: comparison with Korean, Chinese, and Caucasian populations. |
| Nagai et al. (1996) | PKDB00590 | 8830977 | DXM hydrobromide | Oral (tablet): 30 mg | Pharmacokinetics and polymorphic oxidation of dextromethorphan in a Japanese population. |
| Nakashima et al. (2007) | PKDB00599 | 17652181 | DXM hydrobromide | Oral (tablet): 30 mg | Effect of cinacalcet hydrochloride, a new calcimimetic agent, on the pharmacokinetics of dextromethorphan: <i>in vitro</i> and clinical studies. |
| Nyunt et al. (2008) | PKDB00591 | 18362694 | DXM | Oral (tablet): 30 mg | Pharmacokinetic effect of AMD070, an Oral CXCR4 antagonist, on CYP3A4 and CYP2D6 substrates midazolam and dextromethorphan in healthy volunteers. |
| Oh et al. (2012) | PKDB00054 | 22483397 | DXM (in cocktail) | Oral (NR): 2 mg | High-sensitivity liquid chromatography-tandem mass spectrometry for the simultaneous determination of five drugs and their cytochrome P450-specific probe metabolites in human plasma. |
| Pope et al. (2004) | PKDB00592 | 15342614 | DXM | Oral (capsule): 30 mg; 45 mg; 60mg | Pharmacokinetics of dextromethorphan after single or multiple dosing in combination with quinidine in extensive and poor metabolizers. |
| Qiu et al. (2016) | PKDB00600 | 27023460 | DXM hydrobromide | Oral (tablet): 15 mg | Effects of the Chinese herbal formula "Zuojin Pill" on the pharmacokinetics of dextromethorphan in healthy Chinese volunteers with CYP2D6*10 genotype. |
| Schadel et al. (1995) | PKDB00593 | 7593709 | DXM | Oral (capsule): 30 mg | Pharmacokinetics of dextromethorphan and metabolites in humans: influence of the CYP2D6 phenotype and quinidine inhibition. |
| Schoedel et al. (2012) | PKDB00594 | 22283559 | DXM | Oral (capsule): twice daily for 8 days; 30 mg | Randomized open-label drug-drug interaction trial of dextromethorphan/quinidine and paroxetine in healthy volunteers. |
| Tamminga et al. (2001) | PKDB00498 | 11829201 | DXM hydrobromide | Oral (tablet): 22 mg | The prevalence of CYP2D6 and CYP2C19 genotypes in a population of healthy Dutch volunteers. |
| Yamazaki et al. (2017) | PKDB00494 | 27273149 | DXM (in cocktail) | Oral (NR): 30 mg | Pharmacokinetic Effects of isavuconazole coadministration with the cytochrome P450 enzyme substrates bupropion, repaglinide, caffeine, dextromethorphan, and methadone in healthy subjects. |
| Zawertailo et al. (2010) | PKDB00595 | 20041473 | DXM | Oral (capsule): 3 mg/kg | Effect of metabolic blockade on the psychoactive effects of dextromethorphan. |

Table 2. Model parameters in PBPK model of DXM. The complete information is available from the model repository. The prefixes GU__, LI__, KI__, correspond to the intestine/gut, liver, and kidneys, respectively. Values are either adopted from the references or fitted (F). During the robustness analysis of UCMR, various parameters were scanned (S) and a local sensitivity (SA) was performed, see section 3.5.

| Parameter | Description | References | Value | Unit | F | S | SA |
|--------------------|--|---|-----------|------------|---|---|----|
| BW | Body weight | ICRP (2002) (male) | 75 | kg | | | ✓ |
| HEIGHT | Height | ICRP (2002) (male) | 170 | cm | | | ✓ |
| HR | Heart rate | | 70 | 1/min | | | ✓ |
| HRrest | Heart rate (resting) | | 70 | 1/min | | | ✓ |
| COBW | Cardiac output per bodyweight | ICRP (2002); de Simone et al. (1997) | 1.548 | ml/s/kg | | ✓ | ✓ |
| HCT | Hematocrit | Vander (2001); Herman (2016) (upper range male) | 0.51 | - | | | |
| Kp_fo_dex | Tissue/plasma partition coefficient DXM forearm | | 10 | - | | ✓ | ✓ |
| f_shunting_forearm | Shunting in forearm | | 0.2795 | - | | ✓ | |
| FVgu | Gut fractional tissue volume | Jones and Rowland-Yeo (2013); ICRP (2002) | 0.0171 | l/kg | | | ✓ |
| FVki | Kidney fractional tissue volume | Jones and Rowland-Yeo (2013); ICRP (2002) | 0.0044 | l/kg | | | ✓ |
| FVli | Liver fractional tissue volume | Jones and Rowland-Yeo (2013); ICRP (2002) | 0.021 | l/kg | | ✓ | ✓ |
| FVlu | Lung fractional tissue volume | Jones and Rowland-Yeo (2013); ICRP (2002) | 0.0076 | l/kg | | | ✓ |
| FVsp | Spleen fractional tissue volume | Jones and Rowland-Yeo (2013); ICRP (2002) | 0.0026 | l/kg | | | ✓ |
| FVpa | Pancreas fractional tissue volume | Jones and Rowland-Yeo (2013); ICRP (2002) | 0.01 | l/kg | | | ✓ |
| FVfo | Fore arm fractional tissue volume | | 0.0048 | l/kg | | ✓ | ✓ |
| FVve | Venous fractional tissue volume | Jones and Rowland-Yeo (2013); ICRP (2002) | 0.0514 | l/kg | | | ✓ |
| FVar | Arterial fractional tissue volume | Jones and Rowland-Yeo (2013); ICRP (2002) | 0.0257 | l/kg | | | ✓ |
| FVpo | Portal fractional tissue volume | Jones and Rowland-Yeo (2013); ICRP (2002) | 0.001 | l/kg | | | ✓ |
| FQgu | Gut fractional tissue blood flow | Jones and Rowland-Yeo (2013) | 0.146 | - | | | ✓ |
| FQki | Kidney fractional tissue blood flow | Jones and Rowland-Yeo (2013) | 0.19 | - | | | ✓ |
| FQh | Hepatic (venous side) fractional tissue blood flow | Jones and Rowland-Yeo (2013) | 0.215 | - | | | |
| FQlu | Lung fractional tissue blood flow | Jones and Rowland-Yeo (2013) | 1 | - | | | ✓ |
| FQsp | Spleen fractional tissue blood flow | Jones and Rowland-Yeo (2013) | 0.017 | - | | | ✓ |
| FQfo | Fore arm fractional tissue blood flow | RNAO (2022) | 0.0146 | - | | | ✓ |
| FQpa | Pancreas fractional tissue blood flow | ICRP (2002) | 0.017 | - | | | ✓ |
| Mr_dex | Molecular weight DXM | CHEBI:4470 | 271.404 | g/mole | | | |
| ftissue_dex | Vmax tissue distribution DXM | | 1000 | l/min | | ✓ | ✓ |
| Kp_dex | Tissue/plasma partition coefficient DXM | | 8.7346 | - | | ✓ | ✓ |
| Ka_dis_dex | DXM rate of dissolution & stomach passage | | 0.0217 | 1/hr | | ✓ | ✓ |
| Mr_dor | Molecular weight DXO | CHEBI:29133 | 257.3707 | g/mole | | | |
| ftissue_dor | Vmax tissue distribution DXO | | 100 | l/min | | ✓ | ✓ |
| Kp_dor | Tissue/plasma partition coefficient DXO | | 4 | - | | ✓ | ✓ |
| Mr_dor_glu | Molecular weight DXO_glu | CHEBI:32645 | 433.4948 | g/mole | | | |
| ftissue_dor_glu | Vmax tissue distribution DXO_glu | | 3 | l/min | | ✓ | ✓ |
| Kp_dor_glu | Tissue/plasma partition coefficient DXO_glu | | 0.08 | - | | ✓ | ✓ |
| KI__DEXEX_k | DXM urinary excretion rate | | 0.017 | 1/min | | ✓ | ✓ |
| KI__DOREX_k | DXO urinary excretion rate | | 0.3 | 1/min | | ✓ | ✓ |
| KI__DORGLUEX_k | DXO glucuronide urinary excretion rate | | 10 | 1/min | | ✓ | ✓ |
| LI__DEXCYP2D6_Vmax | DXM CYP2D6 Vmax | | 0.003 | mmol/min/l | | ✓ | ✓ |
| LI__DEXCYP2D6_Km | DXM CYP2D6 Km | Storelli et al. (2019a); Yang et al. (2012) | 0.0079 | µM | | | ✓ |
| LI_cyp2d6_ac | CYP2D6 activity score | | 0.0 - 3.0 | - | | | ✓ |
| LI_lambda_1 | Km dimension of the scaled first eigenvector of (Km, Vmax) in log space. | Storelli et al. (2019a); Yang et al. (2012) | -0.4 | - | | ✓ | |
| LI__DEXCYPX_Vmax | Vmax of DXO formation by CYP3A4 | | 0.0004 | mmol/min/l | | ✓ | ✓ |
| LI__DEXCYPX_Km | Km of DXO formation by CYP3A4 | Yu and Haining (2001) | 0.157 | µM | | | ✓ |
| LI__DORUGT_Vmax | DXO UGT Vmax (glucuronidation) | | 0.8953 | mmol/min/l | | ✓ | ✓ |
| LI__DORUGT_Km | DXO UGT Km (glucuronidation) | Lutz and Isoherranen (2012) | 0.69 | µM | | | ✓ |
| GU_F_dex | Fraction absorbed DXM | Schadel et al. (1995) | 0.55 | - | | | ✓ |
| GU_Ka_abs_dex | Ka_abs absorption DXM | | 3.4285 | 1/hr | | ✓ | ✓ |
| GU__DEXCYP3A4_Vmax | DXM CYP3A4 Vmax | | 0.0002 | mmol/min/l | | ✓ | ✓ |
| GU__DEXCYP3A4_Km | DXM CYP3A4 Km | Kerry et al. (1994); Yu and Haining (2001) | 0.7 | µM | | | ✓ |
| PODOSE | DXM oral dose | | | mg | | ✓ | ✓ |